SESSION 5.

APPLICATIONS

Session Chairman

W. Lansing

Grumman Aircraft Engineering Corp.
Bethpage, New York

ANALYSIS OF THE 747 AIRCRAFT WING-BODY INTERSECTION

S. D. Hansen,* G. L. Anderton,**
N. E. Connacher,*** C. S. Dougherty,****
The Boeing Company, Renton, Washington

To provide accurate internal loads information in the 747 wing-body intersection area, a redundant analysis was performed using finite element theory and matrix algebra. The structure, idealized as four substructures containing a total of 4,266 nodes and 12,549 elements, was analyzed on a CDC 6600 computer using company-developed force and direct stiffness analysis programs coupled with a flexibility-type interaction program. Flexibility matrices and non-interacted deflections for the interacting freedoms of each substructure were merged into a fully cross-coupled set of interaction equations. The equations thus formed were solved for the unknown interaction forces required for the calculation of final stresses and deflections. The solution was formulated for a set of generalized unit loadcases which could be factored and combined into a solution for real load-cases. This paper is a description of a successful application of finite element and interaction theory to an unusually large problem in air-craft production design and is not intended as a treatise on the theory involved.

*Research Engineer, Commercial Airplane Division
**Design Specialist, Commercial Airplane Division
***Associate Research Engineer, Commercial Airplane Division
****Structures Engineer, Commercial Airplane Division

SECTION I

INTRODUCTION

The wing-body intersection of the 747 aircraft is an area of considerable complexity and, consequently, a redundant analysis was necessary in order to predict the internal loads distribution accurately. The region of the aircraft analyzed included 1000 inches of fuselage, the wheel-well area, and the wing primary structure out to a point midway between the engines. Since the size of the total problem far exceeded the capabilities of both existing programs and computers, the structure was divided into four substructures.

The analysis was performed on the CDC 6600 computer using both the force method and the direct stiffness method combined into an integrated analysis system. The system is completely modular, with full recoverability provided at the interface of each module. Many automatic checking features are included for both data input and program output.

Internal loads and deflections of the full structure were found by mathematically connecting the four substructures using a flexibility interaction concept. The flexibility matrices and noninteracted deflections of the interacting freedoms for each substructure were automatically formed into a fully cross-coupled set of simultaneous equations by enforcing compatibility across the substructure interfaces. The equations were then solved for the unknown interaction forces, which were subsequently applied to the individual substructures.

A significant feature of this analysis was the formation of stresses and deflections for a set of generalized unit loadcases. By scaling and combining the results of the generalized unit solutions, stresses and deflections for any real loadcases can be obtained at any time — an automated procedure of nearly negligible cost.

This analysis was completed over a 10-month period and represents the largest of several similar analyses performed in the last several months. Some general interest information concerning two of these other projects is included as an appendix.

SECTION II

PROBLEM DEFINITION

The region analyzed included the wing-body intersection of the 747 aircraft, shown shaded in Figure 1, and consisted of all of the monocoque from B.S. (body station) 680 aft to B.S. 1740 and all of the wing box structure between right and left B.L. (buttock line) 688. This analysis is identified as 747-4 to distinguish it from previous similar analyses made of the same region.

Two previous finite element analyses of the 747 wing-body intersection have been completed. The first, designated 747-2, was completed in the summer of 1966 and consisted of a very coarse grid of the fuselage and wing center section in order to determine major load paths for initial sizing. The second, designated 747-3, was completed at the end of 1966 and used directly for design. It consisted of a 1000-node wing substructure and a 1500-node fuselage substructure. The wing substructure for 747-3 was idealized in essentially the same manner as for the analysis being discussed in this paper. The frame grid of the fuselage for the three analyses performed is shown in Figure 2. Note that the frame grid was refined by a factor of approximately two for each successive analysis. The stringer grid in all cases was determined by lumping an average of three real stringers into one idealized stringer.

All analyses of this region have been performed to obtain overall load distributions and to obtain specific, detailed information concerning the following items:

- The induced bending effects of the wing on the fuselage frames at the side of the body
- The effect of wing bending on the landing gear beam (the landing gear beam is pinned at the attachment to the wing rear spar but fixed at the side of the body)
- The effects of the stresses induced into the pressure deck (see Figure 5) as the result of wing bending and the subsequent shortening of the upper chord of the rear spar
- The distribution of loads in the area of the discontinuity caused by the wheel-well cutout
- The distribution of landing gear loads into the supporting bulkheads and monocoque structure
- The distribution of floor loads in the redundant floor-grid structure

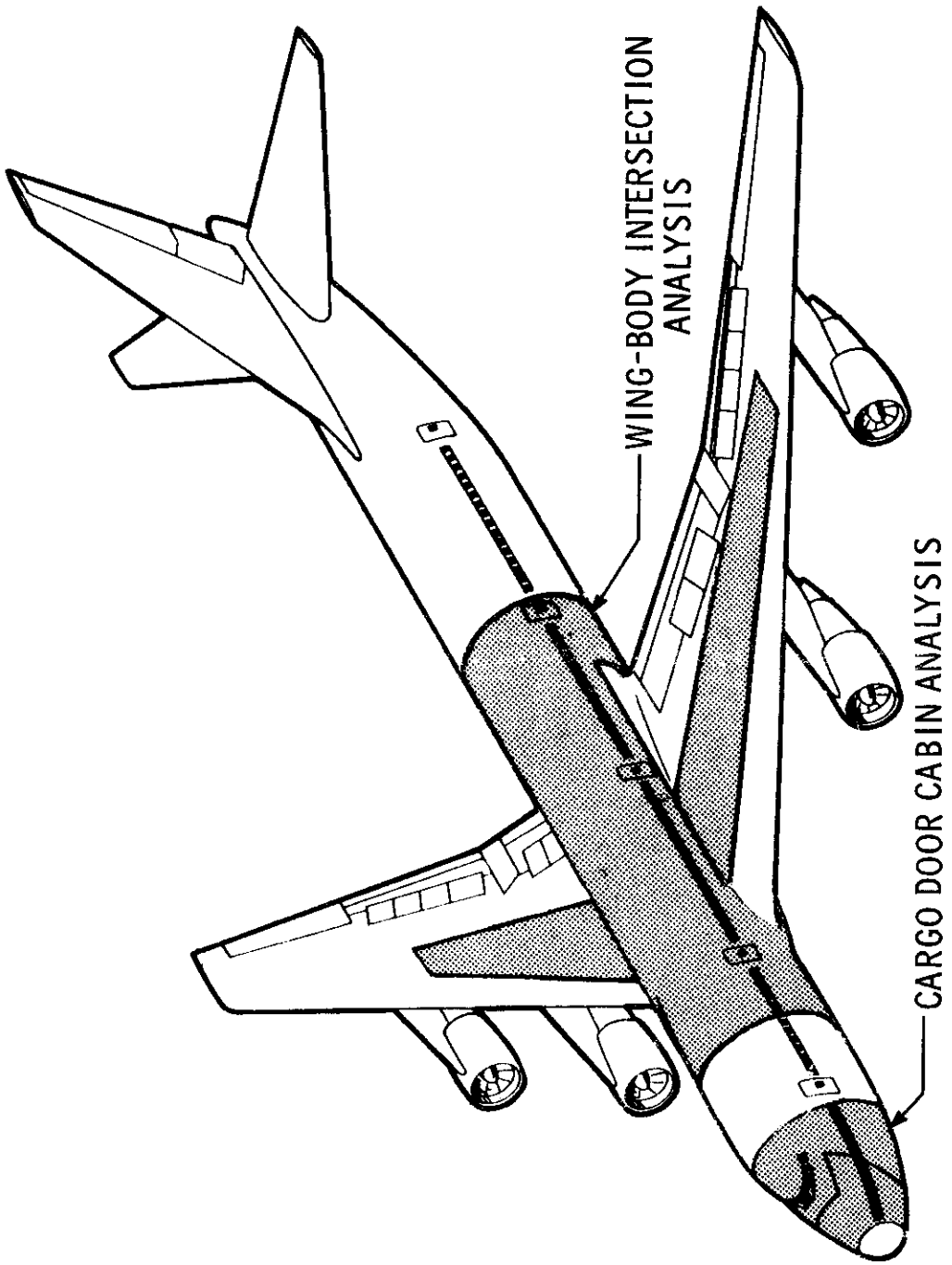

Figure 1. 747 Regions Analyzed

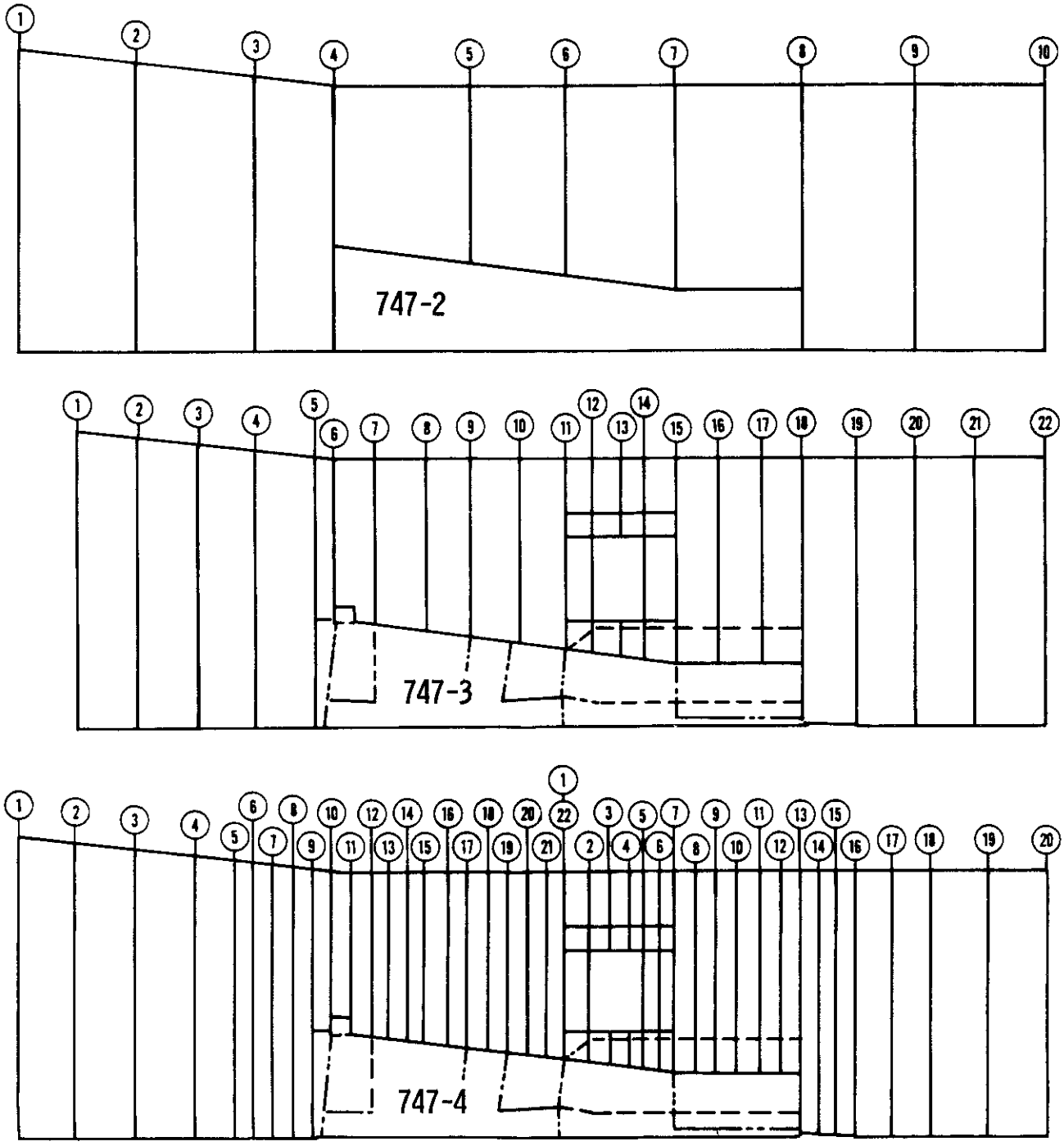

Figure 2. History of Analysis

The region was divided into the following four major substructures, shown schematically in Figure 3.

Substructure A — B.S. 680 aft to B.S. 1238

Substructure B — B.S. 1238 aft to B.S. 1740 (this substructure included the aft wheel-well bulkhead at B.S. 1480)

Substructure C — Wing primary structure between right and left B.L. 688 including the wing center section and the front, mid and rear spar bulkheads

Substructure D — Wheel-well area including the landing gear beams and trunnions, mid wheel-well bulkhead, pressure deck, torque boxes, and keel beam

The choice of substructure interfaces was based mainly upon the following considerations:

- Division of the structure according to group responsibility for design
- Division of responsibility between subcontractor and prime contractor
- Computer program and hardware capacity and reliability considerations
- Major assembly components (production breaks)

The use of substructures in the analysis of the region had the added advantages of allowing parallel preparation and processing of data and permitting communication between subcontractor and prime contractor in a precise and mutually understood form.

LOADING

A significant feature of this analysis was the effective use of the concept of generalized unit loads. Solution of the problem for unit loads in the usual manner (i.e. application of a load value of one at each load point as separate loadcases) would have far exceeded the capacity of both programs and computer. Instead, generalized unit loadcases were formed by dividing the structural loading into 169 individual loading cases which could be effectively scaled and combined to form all actual loadcases of practical interest. As an example, one generalized loadcase consisted of a 10,000-lb cargo loading distributed over the floor beams

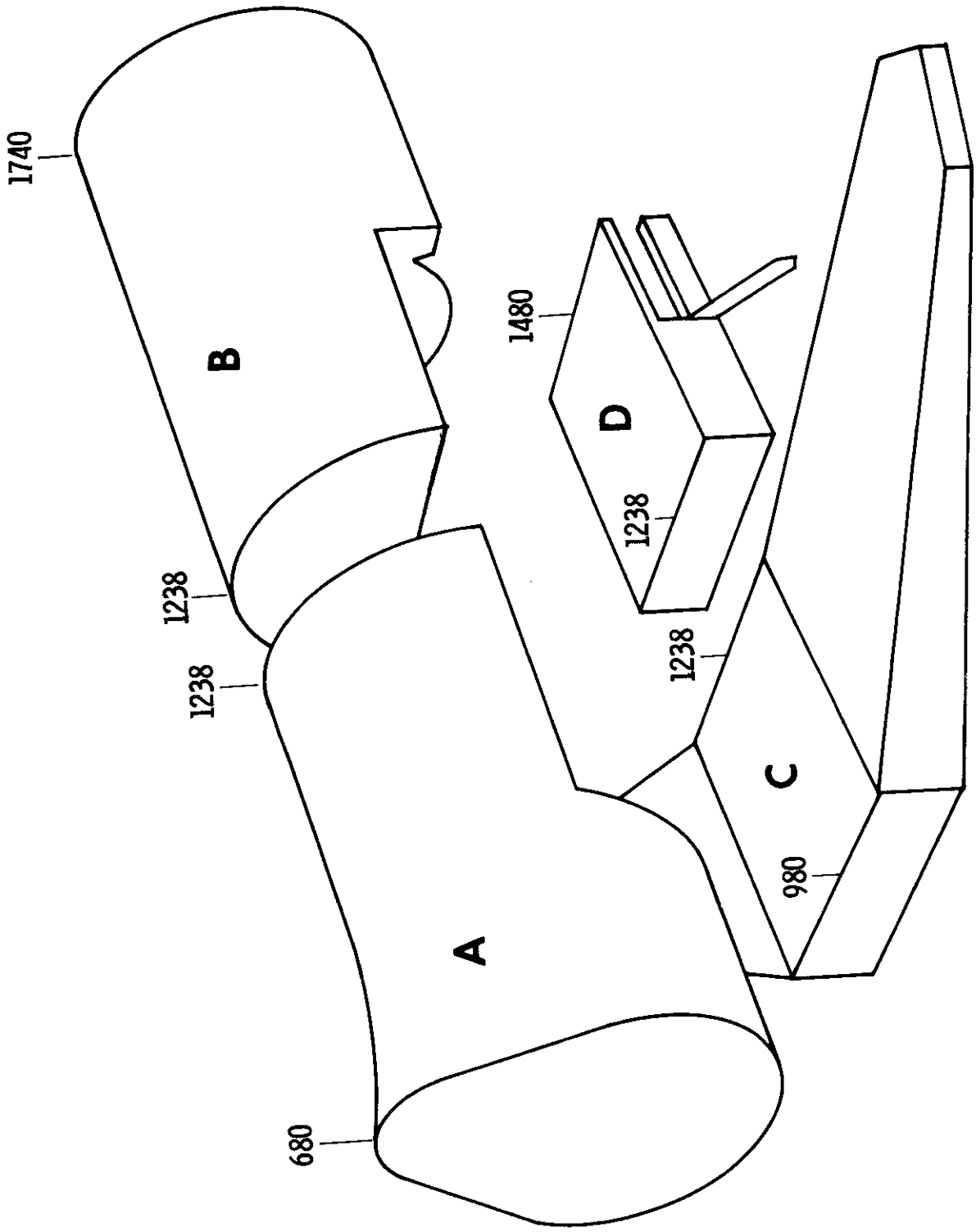

Figure 3. Schematic of Substructures

at four stations. Another consisted of the application of a 10,000,000-in.-lb torque at the aft monocoque boundary. Still others consisted of 1-lb loads applied at node points along the wing surface. Continuing in this manner loadcases were defined which, when appropriately scaled and combined, adequately described the structural loading due to pressure, airloads, inertia, cargo, or any combination of these.

A major reason for adopting this procedure is that, following the usual procedure, a finite element analysis cannot proceed until the loads have been defined. In aircraft design, the external applied loads usually lag the structural configuration by a significant length of time. However, using the generalized unit loads concept, the analysis could be completed while applied loads were being determined. The data required for applied loads, then, consisted of a matrix of scaling and combining factors for the substructure stresses and deflections already determined using the generalized unit loading cases.

A second reason for adopting this procedure is that, since the results are stored indefinitely on magnetic tape, stresses and deflections can be quickly formed for loadcases not anticipated or available originally. Hence, the results of the analysis can be used until changes in the structure become severe enough to make the original structural data used in the analysis obsolete. Further, results for new loadcases, which are inevitably required on a priority basis, can be obtained quickly enough to be useful.

IDEALIZATION OF SUBSTRUCTURES

Substructures A and B were idealized to include primary and secondary door sills, floors, intercostals, and body crease beams (Figure 4). The aft wheel-well bulkhead in Substructure B was idealized separately and treated as a superelement. To provide plane-section boundary conditions, the first bay of Substructure A and the last bay of Substructure B were made rigid.

A study of the results from the 747-3 analysis had shown that the stress gradients in the wing-body joint area were extremely large. Hence, the averaging effect of the finite element method coupled with the frame lumping used in the 747-3 analysis produced results for this area which were unsatisfactory for direct use in detailed design. To correct this in the 747-4 analysis, every frame was included for the over-wing and over-wheel-well areas. For the same reason, the stringer grid was refined on the bottom of the monocoque to include every stringer.

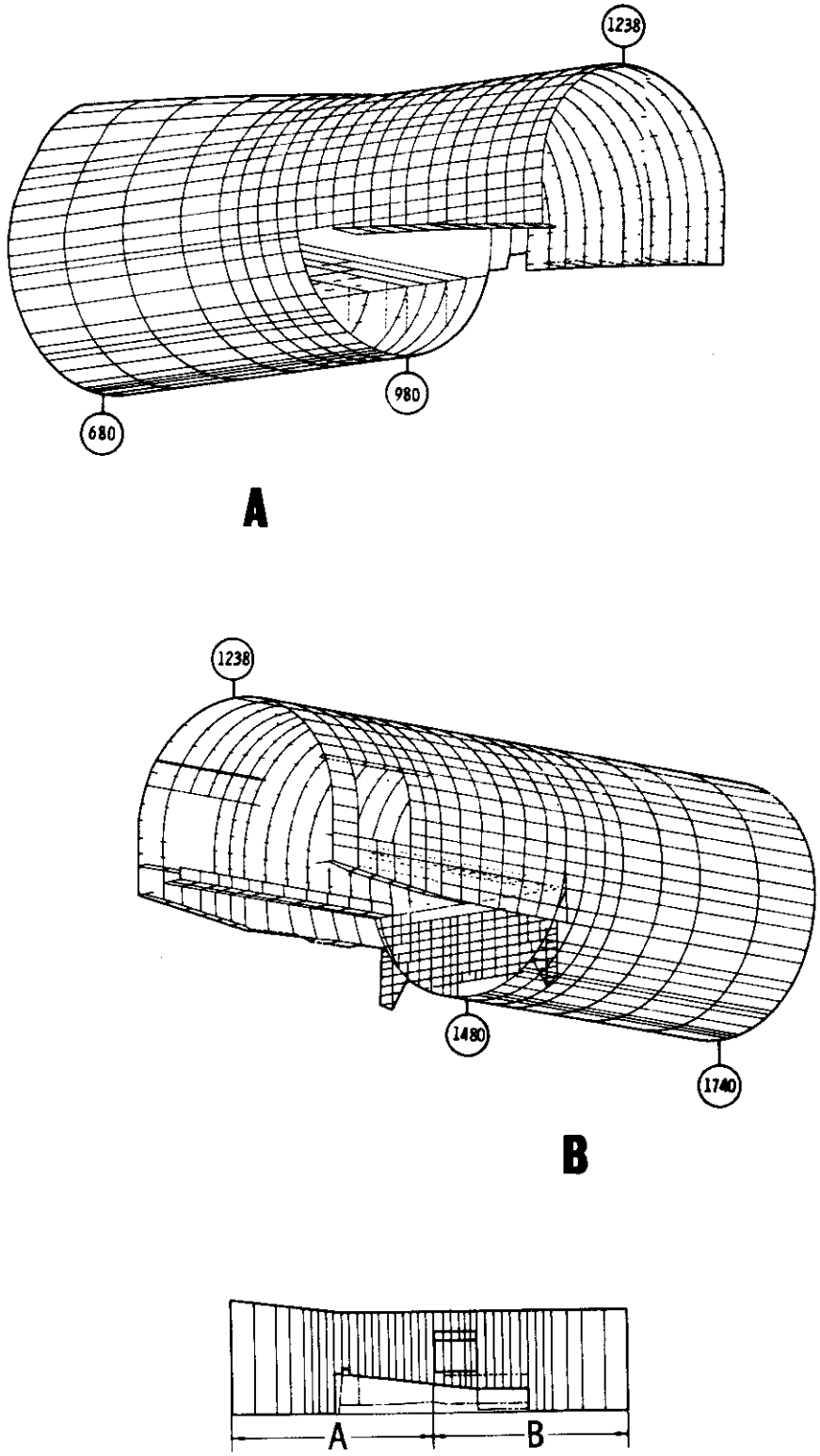

Figure 4. Monocoque Idealization

The four frames directly forward of the front spar bulkhead at B.S. 980 and the three frames directly aft of the rear wheel-well bulkhead at B.S. 1480 were included to provide good definition in those regions where the wing front spar and the keel beam structure, respectively, were spilling high loads into the monocoque. The frame grid was coarsened beyond these points as the idealization approached the boundaries of the region analyzed.

The monocoque skin panels were idealized as pure shear fields with the in-plane stretching capacity lumped into the adjoining stringer and frame elements. Stringers were idealized as rod members with axial stiffness only. Frames were idealized as offset beams with axial stiffness and shear and moment stiffness in the plane of the frame. Longitudinal bending members were built up from axial flanges connected by shear webs.

Substructures C and D were idealized as symmetric half structures, as shown in Figure 5. Symmetric and antisymmetric boundary conditions, respectively, were imposed at the centerline nodes and half structure flexibility and deflection matrices were formed. The flexibility and deflection matrices thus obtained were merged to form the flexibility and deflection matrices for the full structure. This procedure was chosen for the following reasons.

- The direct stiffness program used was just being implemented on the CDC 6600 computer and was only considered reliable for a problem size of about a half structure.
- Analyzing the half structure, while doubling the number of processing runs, decreased the size of the structure being analyzed, and thus the amount of input data to one-half.
- The merging of the symmetrical and antisymmetrical matrices was a very minor task; hence, the net effect of using half structures was a reduction of computer costs and easier access to the computer because of the smaller problem size.

Substructure C was idealized to include the front, mid, and rear spars, and every rib. Four actual stiffeners were lumped to one idealized stiffener.

Substructure D consisted of a variety of components, as shown in Figure 5. It was idealized using a grid consistent with the adjoining substructures.

Skin panels in substructures C and D were idealized using constant strain isotropic plate elements with in-plane shear and membrane stiffness. Out-of-plane effects were considered negligible. Spars and ribs were idealized using beam elements as flanges and shear plates as webs. Stiffeners were idealized as beams with axial, shear, and bending stiffness.

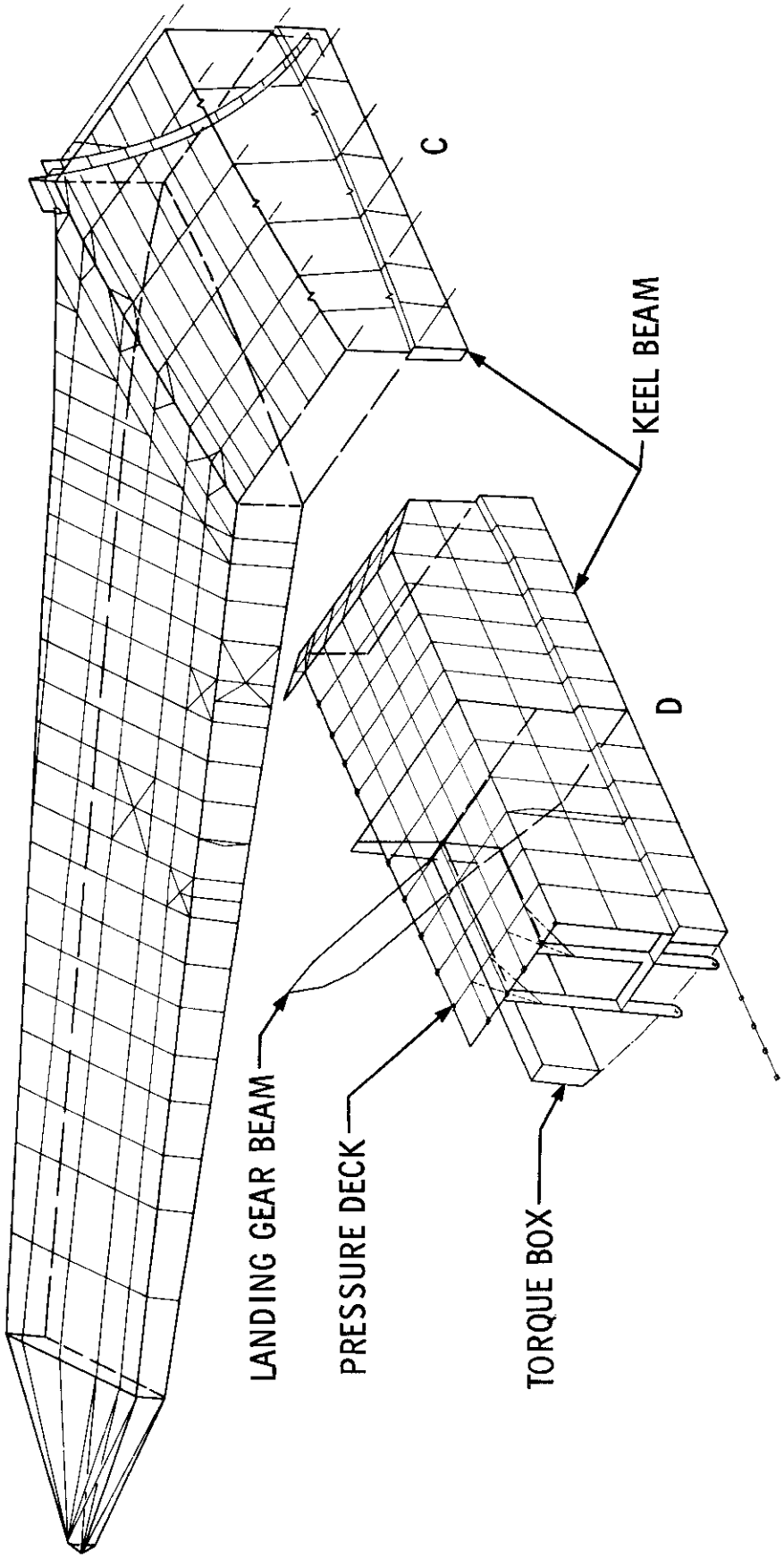

Figure 5. Wing and Wheel-Well Area Idealization

The substructure interfaces were idealized to interact those freedoms that represented the major load paths between substructures. In general either one, two, or three translational freedoms were interacted at each node. Rotational freedoms were interacted in the direction of the principal bending axis of interfacing beams.

Substructure statistics are summarized in the following table.

Substructure	Nodes	Elements	Simultaneous Equations
A	1,009	2,897	1,003
B	1,014	2,728	1,017
C*	1,060	3,546	~6,000
D*	894	2,526	~5,000
Aft wheel-well bulkhead**	289	852	~ 850
Totals	4,266	12,549	13,870

The following list gives the number of interaction freedoms for each interface.

Interface	Interacted Freedoms
A-B	85
A-C*	200
B-D*	195
C-D*	73
Aft wheel-** well bulkhead - B	156
Total	709

* Full structure

**Super element for substructure B

SECTION III

GENERAL STRUCTURAL ANALYTICAL PROGRAMS

DESCRIPTIONS OF SYSTEMS

Four general structural analytical programs were used in this project.

- FUSARG — A multiple-run group of interfacing programs developed around the force method approach to the analysis of redundant structures. This group of programs was developed specifically for the analysis of monocoque structures (Reference 1) and is capable of producing all information required for flexibility-type interaction problems.

- CHEDIP — A direct stiffness program (Reference 2) developed specifically to analyze monocoque bulkheads and produce the required information for treatment of the bulkheads as super elements by FUSARG. Interfacing with FUSARG is completely automatic for both the transfer of flexibilities to FUSARG and the transfer of loads from FUSARG for determination of bulkhead internal loads and deflections.

- SAMECS — A direct stiffness program (Reference 2) designed for single-run analyses of linear structures. This program was not designed to interface with the other analysis programs and required modification for this project. Flexibility matrices required for interaction were produced by assembling and sorting the deflections resulting from the application of a unit load at each interaction freedom.

- FLINT — A flexibility interaction program (Reference 3) developed specifically for use on this project. The program is general, however, and may be used for a wide variety of interaction problems. It interfaces directly with FUSARG and SAMECS to receive information required for interaction and return information required from interaction for determination of interacted internal loads and deflections for each substructure.

All data transfer between programs is automatic. Magnetic tape provides intermediate storage of data between processing periods and long-term storage of results. Recovery of data from tapes proved to be the least reliable facet of the entire operation and was by far the greatest cause of delay in completing the project.

The analysis system combined these four major program groups in a modular fashion to provide:

- Adequate recovery capability from computer software error or hardware failure;
- Subtask processing with computing storage and residency times consistent with the capacity and reliability of existing programs and hardware;
- Opportunity for checks on the processing at sufficient intermediate points to discover and correct errors at the earliest point possible.

The collection of modules necessary to process a subtask is called a stage. Figure 6 is a staging diagram and represents the general processing flow. The actual staging diagrams used for the project were more detailed than those shown; however, those shown represent the general organization of the system for this project.

Recovery is possible at each stage interface. Stages requiring lengthy processing or involving several distinct operations have recovery capability at one or more points with the stage. As a general rule, recovery is provided so that maximum required residency on the CDC 6600 computer is restricted to five hours or less. The system is designed so that essential input data is not destroyed within any stage unless duplicate tapes have been generated which contain that input data. Hence, sufficient information is always available for re-processing of any stage.

Automated checking features in the system include:

- Node point coordinate plotting;
- Computation and plotting of shear, moment, and torque diagrams for external applied loads and internal element loads;
- Compatibility checks;
- Equilibrium checks;
- Matrix conditioning checks.

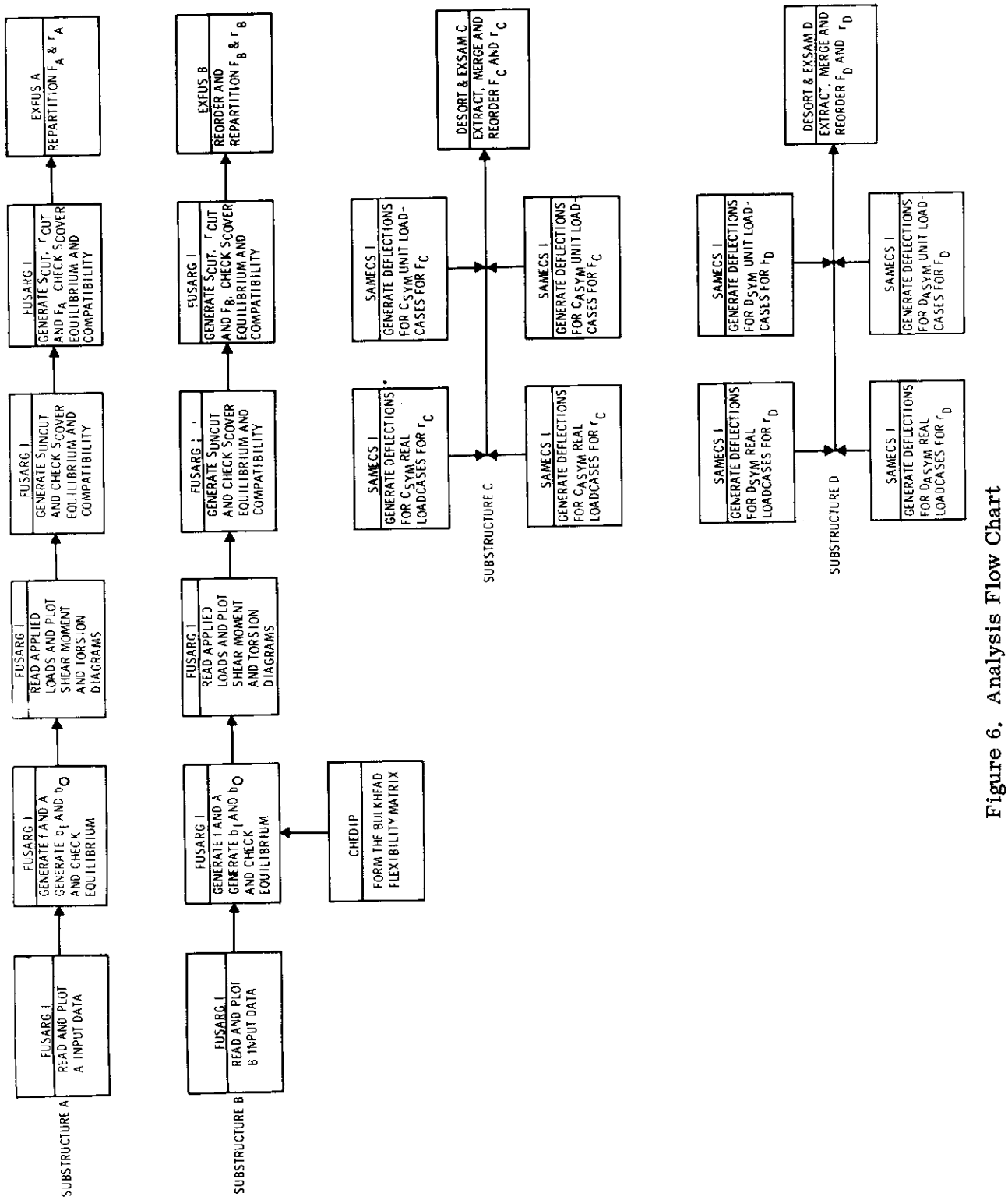

Figure 6. Analysis Flow Chart

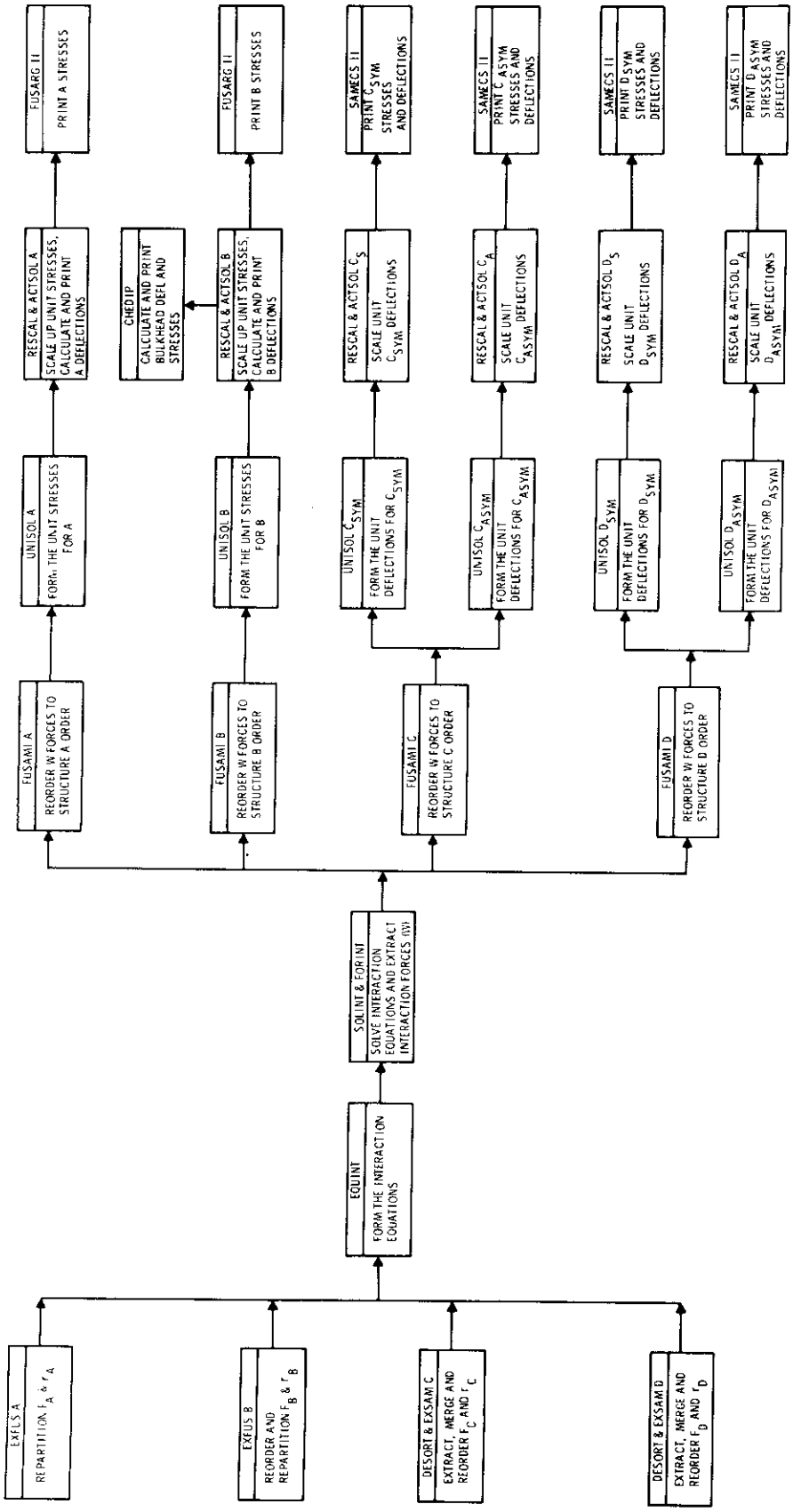

Figure 7. Analysis Flow Chart

Intermediate results are printed by the system, either automatically or optionally, to aid the analyst in checking the logical and numerical correctness of the processing. Management control requires that sufficient checks be performed on these intermediate results so that the final delivered results can be verified as correct.

FLINT ANALYSIS PROCEDURE

The heart of the interaction system is the FLINT program. The basic theory used by the FLINT interaction program represents no new development. The main difficulty with this program, as with much finite element work, was not the development of the theory but rather the translation of the theory into an operational, production-oriented data processing system. Hence, only an example of the theory as it applies to this particular project has been included in this paper.

The overall function of the FLINT program is to form and solve the equation:

$$\mathbf{F}\,\mathbf{W} = \mathbf{r} \qquad (1)$$

where:

$\mathbf{F}$ = known, ordered sum of all substructure flexibility matrices

$\mathbf{W}$ = unknown set of self-equilibrating interaction forces necessary to enforce deflection compatibility across the substructure interfaces

$\mathbf{r}$ = known set of deflections, or gaps, between interacting freedoms on the substructure interfaces prior to interaction

The main difficulty is the formation of the $\mathbf{F}$ and $\mathbf{r}$ arrays and the sorting of the resultant $\mathbf{W}$ forces for application back on the appropriate substructures. The FLINT program has been designed to simplify these operations. The solution of the equation, once formed, is trivial.

To illustrate the FLINT program theory, the 747 interaction problem, shown schematically in Figure 8, will be used. A more basic discussion of interaction theory may be found in References 1 and 3.

In Figure 8, the forces $\mathbf{W}_{02}$ form the statically determinate primary support system for substructures A and B and the deflection reference datum plane for the entire structure.

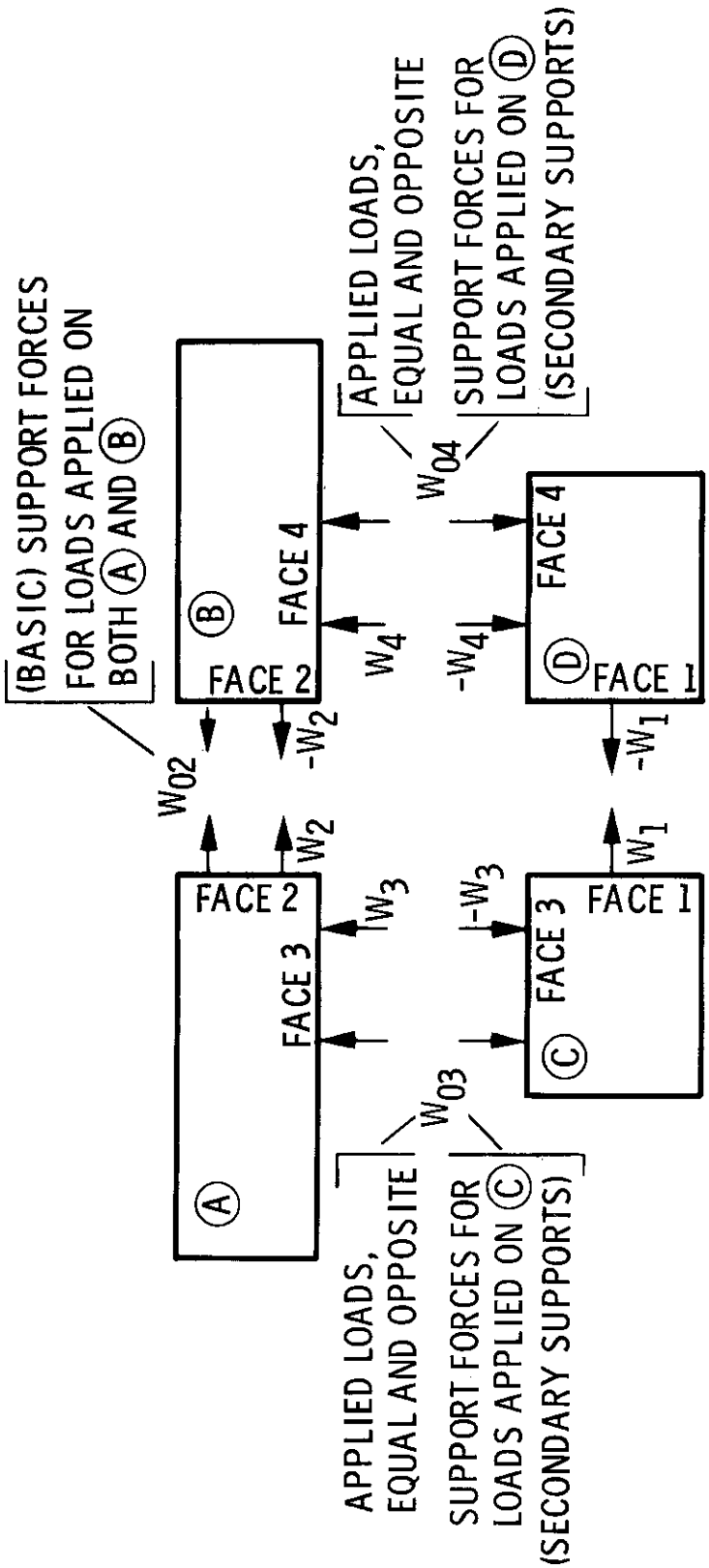

Figure 8. 747 Interaction Problem Schematic

The secondary supports, W_{03} and W_{04}, are the statically determinate support systems for substructures C and D respectively, and are also the local deflection datum planes for these substructures. The forces W_1, W_2, W_3 and W_4 are the unknown, redundant, self-equilibrating forces to be determined from the interaction equation.

The general procedure is to solve each of the substructures separately for the substructure flexibility and deflection matrices. These matrices are then sorted to include only those terms associated with the interacting freedoms, and ordered in preparation for merging to form the interaction equation.

The interaction flexibility matrix for substructure A is obtained from FUSARG in the form:

$$F_A = \begin{bmatrix} A_{2,2} & A_{2,3} & A_{2,03} \\ A_{3,2} & A_{3,3} & A_{3,03} \\ A_{03,2} & A_{03,3} & A_{03,03} \end{bmatrix}$$

where

$A_{2,2}$ = deflections of interacted freedoms on face 2 of A due to unit W_2 forces (relative to primary statics)

$A_{2,3}$ = deflections of interacted freedoms on face 2 of A due to unit W_3 forces (relative to primary statics)

$A_{2,03}$ = deflections of interacted freedoms on face 2 of A due to unit W_{03} forces (relative to primary statics)

$A_{3,2}$ = deflections of interacted freedoms on face 3 of A due to unit W_2 forces (relative to secondary statics)

$A_{3,3}$ = deflections of interacted freedoms on face 3 of A due to unit W_3 forces (relative to secondary statics)

$A_{3,03}$ = deflections of interacted freedoms on face 3 of A due to unit W_{03} forces (relative to secondary statics)

$A_{03,2}$ = deflections of secondary statics on A due to unit W_2 forces (relative to primary statics)

$A_{03,3}$ = deflections of secondary statics on A due to unit W_3 forces (relative to primary statics)

$A_{03,03}$ = deflections of secondary statics on A due to unit W_{03} forces (relative to primary statics)

The interaction flexibility matrix for substructure B is obtained from FUSARG in the form:

$$F_B = \begin{bmatrix} B_{2,2} & B_{2,4} & B_{2,04} \\ B_{4,2} & B_{4,4} & B_{4,04} \\ B_{04,2} & B_{04,4} & B_{04,04} \end{bmatrix}$$

The terms in this matrix have meanings similar to those given for substructure A.

The interaction flexibility matrix for substructure C after the symmetric-asymmetric merge is of the form:

$$F_C = \begin{bmatrix} C_{1,1} & C_{1,3} \\ C_{3,1} & C_{3,3} \end{bmatrix}$$

where

$C_{1,1}$ = deflections of interacted freedoms on face 1 of C due to W_1 forces (relative to secondary statics)

$C_{1,3}$ = deflections of interacted freedoms on face 1 of C due to W_3 forces (relative to secondary statics)

$C_{3,1}$ = deflections of interacted freedoms on face 3 of C due to W_1 forces (relative to secondary statics)

$C_{3,3}$ = deflections of interacted freedoms on face 3 of C due to W_3 forces (relative to secondary statics)

Similarly, the interaction flexibility matrix for substructure D is of the form:

$$F_D = \begin{bmatrix} D_{1,1} & D_{1,4} \\ D_{4,1} & D_{4,4} \end{bmatrix}$$

The following load transformation matrices are required in order to obtain the deflections of the substructures relative to a common base. For substructure C:

$c_{03,1}$ = loads at the secondary supports (W_{03}) due to unit loads at face 1 (W_1)

$c_{03,0}$ = loads at the secondary supports (W_{03}) due to applied loads on substructure C or at the supports of C (thus enabling the loading of the secondary supports)

$c^T_{03,1}$ = displacements at face 1 due to unit displacements of the secondary supports at face 3.

Similarly, for substructure D:

$$d_{04,1}, \quad d_{04,0}, \quad d^T_{04,1}$$

Initial deflections of the unconnected structures due to applied loads are also calculated for the four substructures as part of the preparation of interaction. For substructure A, these are:

r^A_2 = deflections of interacted freedoms on face 2 due to applied loads on A (relative to primary supports)

r^A_3 = deflections of interacted freedoms on face 3 due to applied loads on A (relative to secondary supports)

r^A_{03} = deflections of the secondary supports due to applied loads on A (relative to primary supports

Similarly, for substructures B, C, and D the terms are, respectively:

$$r^B_2, \quad r^B_4, \quad r^B_{04}, \quad r^C_1, \quad r^C_3, \quad r^D_1, \quad r^D_4$$

Having defined these terms, it is possible to set up the equation of compatibility for each interaction face. For face 1:

$C_{1,1}W_1$ = deflections of face 1 freedoms due to interaction forces on face 1 (relative to secondary statics)

$C_{1,3}(-W_3)$ = deflections of face 1 freedoms due to interaction forces on face 3 (relative to secondary statics)

$(-c^T_{03,1})\ A_{03,03}\ (c_{03,1})\ W_1$

loads on secondary supports due to interaction forces on face 1

deflections of secondary supports due to loads on secondary supports (relative to primary supports)

deflections of face 1 due to loads on secondary supports (relative to primary supports)

$(-c^T_{03,1})\ A_{03,2}\ W_2$

deflections of secondary statics due to interaction forces on face 2 (relative to primary statics)

deflections of face 1 due to deflections of secondary statics, due to interaction forces on face 2 (relative to primary statics)

$(-c^{T}_{03,1})\ A_{03,3}\ W_3$

deflections of secondary statics due to interaction forces on face 3 (relative to primary statics)

deflections of face 1 due to deflections of secondary statics in turn due to interaction forces on face 3 (relative to primary statics)

$(-c^{T}_{03,1})\ r^{A}_{03}$ = deflections at secondary supports due to applied loads on A, transformed to deflections on face 1 (relative to primary statics)

$(-c^{T}_{03,1})\ A_{03,03}\ c_{03,0}$

loads at the secondary supports due to applied loads on substructure C

deflections of secondary supports due to loads on the secondary supports (relative to primary statics)

deflections at interacted freedoms on face 1 due to loads on the secondary supports (relative to primary statics)

The above terms are all of the deflection contributions at face 1 referenced to the basic supports W_{02}. Similar terms exist for deflections of substructure D on face 1. Assembling these terms into the equation for compatibility at face 1 produces:

$$C_{1,1}\ W_1 + C_{1,3}(-W_3) + r_1^C + (-c_{03,1}^T)\ A_{03,03}(-c_{03,1})\ W_1$$
$$+ (-c_{03,1}^T)\ A_{03,2}\ W_2 + (-c_{03,1}^T)\ A_{03,3}\ W_3 + (-c_{03,1}^T)\ r_{03}^A$$
$$+ (-c_{03,1}^T)\ A_{03,03}\ c_{03,0}$$
$$= D_{1,1}(-W_1) + D_{1,4}(-W_4) + r_1^D + (-d_{04,1}^T)\ B_{04,04}(-d_{04,1})(-W_1)$$
$$+ (-d_{04,1}^T)\ B_{04,2}(-W_2) + (-d_{04,1}^T)\ B_{04,4}\ W_4 + (-d_{04,1}^T)\ r_{04}^B$$
$$+ (-d_{04,1}^T)\ B_{04,04}\ d_{04,0} \qquad (2)$$

Similiar but less complicated equations exist for the other three faces.

For face 2:

$$A_{2,2}\ W_2 + A_{2,3}\ W_3 + A_{2,03}(-c_{03,1})\ W_1 + r_2^A + A_{2,03}\ c_{03,0}$$
$$= B_{2,2}(-W_2) + B_{2,4}\ W_4 + B_{2,04}(-d_{04,1})(-W_1) + r_2^B + B_{2,04}\ d_{04,0} \qquad (3)$$

for face 3:

$$A_{3,3}\ W_3 + A_{3,2}\ W_2 + r_3^A + A_{3\,03}(-c_{03,1})\ W_1 + A_{3,03}\ c_{03,0}$$
$$= C_{3,3}(-W_3) + C_{3,1}\ W_1 + r_3^C \qquad (4)$$

and for face 4:

$$B_{4,4}\ W_4 + B_{4,2}(-W_2) + r_4^B + B_{4\,04}(-d_{04,1})(-W_1) + B_{4,04}\ d_{04,0}$$
$$= D_{4,4}(-W_4) + D_{4,1}(-W_1) + r_4^D \qquad (5)$$

Equations 2, 3, 4, and 5 are then solved for the interaction forces W_1, W_2, W_3 and W_4.

The apparent complexity of the above equations is deceiving. The actual formation of the equations is simply done, as can be seen from Equation 6.

$$
\begin{bmatrix}
C^T_{03,1}A_{03,03}C_{03,1} + d^T_{04,1}B_{04,04}d_{04,1} + C_{1,1} + D_{1,1} & -C^T_{03,1}A_{03,2} - d^T_{04,1}B_{04,2} & -C^T_{03,1}A_{03,3} - C_{1,3} & d^T_{04,1}B_{04,4} + D_{1,4} \\
-A_{2\,03}C_{03\,1} - B_{2,04}d_{04,1} & A_{2,2} + B_{2,2} & A_{2,3} & -B_{2,4} \\
-A_{3,03}C_{03,1} - C_{3,1} & A_{3,2} & A_{3,3} + C_{3,3} & 0 \\
B_{4,04}d_{04,1} + D_{4,1} & -B_{4,2} & 0 & B_{4,4} + D_{4,4}
\end{bmatrix}
\times
\begin{bmatrix} W_1 \\ W_2 \\ W_3 \\ W_4 \end{bmatrix}
=
\begin{bmatrix}
C^T_{03,1}(A_{03,03}C_{03,0} + r^A_{03}) - d^T_{04,1}(B_{04,04}d_{04,0} + r^B_{04}) - r^C_1 + r^D_1 \\
-A_{2,03}C_{03,0} - r^A_2 + B_{2,04}d_{04,0} + r^B_2 \\
-A_{3,03}C_{03,0} - r^A_3 + r^C_3 \\
-B_{4,04}d_{04,0} - r^B_4 + r^D_4
\end{bmatrix}
\qquad (6)
$$

Equation 6 is Equation 1 in expanded form and represents Equations 2, 3, 4, and 5 in combined or matrix form. The equation is partitioned by interface, as indicated by the term subscripts. Each partition in the matrix is the sum of all of the contributing partitions from F_A, F_B, F_C, and F_D appropriately transformed to compatible reference bases. Hence, the first row of partitions in Equation 6 consists of the sum of the original terms of the substructure flexibility and deflection matrices, premultiplied by appropriate transformation matrices. Similarly, the first column of partitions consists of the sum of the original substructure flexibility matrices which have been postmultiplied by the appropriate transformation matrices.

Following solution of the interaction equation, the interaction forces, W, are applied to each substructure and the resulting interacted stresses and deflections are determined.

IMPLEMENTATION OF ANALYSIS

To perform the analysis, a team was formed composed as follows:

- Two members from the 747 Stress group, responsible for:
  - Idealization of the substructures
  - Preparation of structural data
  - Preparation of loads data
  - Checking of computer output that was structure oriented
- Two members from the Stress Analysis Research group, responsible for:
  - General consulting to ensure that the idealization was consistent with program theory
  - Processing of data requiring use of released production programs
  - Checking of intermediate computer output to ensure correct functioning of program and computer
  - General team coordination of the project
- Two members from the Structures Programming group, responsible for:
  - Development of new programs
  - Processing of data requiring use of programs not released for production work
  - Checking of program-oriented computer output to ensure correct functioning of program and computer
  - General consulting on program and computer characteristics

The division of responsibility, though generally maintained, was not strict and team members functioned wherever individual talents could be best applied. Additional staff was assigned to the team as required. The maximum staff assigned to the project at any one time was approximately 30.

TASK ORGANIZATION AND SCHEDULING

The project was divided into a sufficient number of subtasks to clearly identify each data handling operation. A PERT-type task organization chart was created, generally following the outline of the staging diagrams shown in Figures 6 and 7.

Scheduling was also established for the project on a subtask level. Whereas the task organization chart established the logical relationship of the subtasks, the scheduling chart (Figure 9) established their calendar relationship. Each major activity is calendar-sequenced on a time line, which was based upon:

- The estimated amount of time required to complete each subtask
- The required completion date of each subtask in order that the output from the subtask be available for use by dependent subtasks

Data processing goals were established based upon scheduled delivery of error-free data and error-free processing of this data.

The task organization chart and the scheduling chart were used together to identify the order in which the tasks were to be done and to provide visibility of subtasks that were causing delay so that corrective action could be taken. Both charts were completed before the project was started in order to ensure that all details had been considered and that computing facilities would be available for the large blocks of time required.

Some delays were encountered during the processing requiring modification of the schedule and, as the project progressed, desirable changes were made to the task organization chart. In general however, the project proceeded as initially planned. The successful completion of the project was the direct result of the thorough and concentrated effort spent in the initial planning phase.

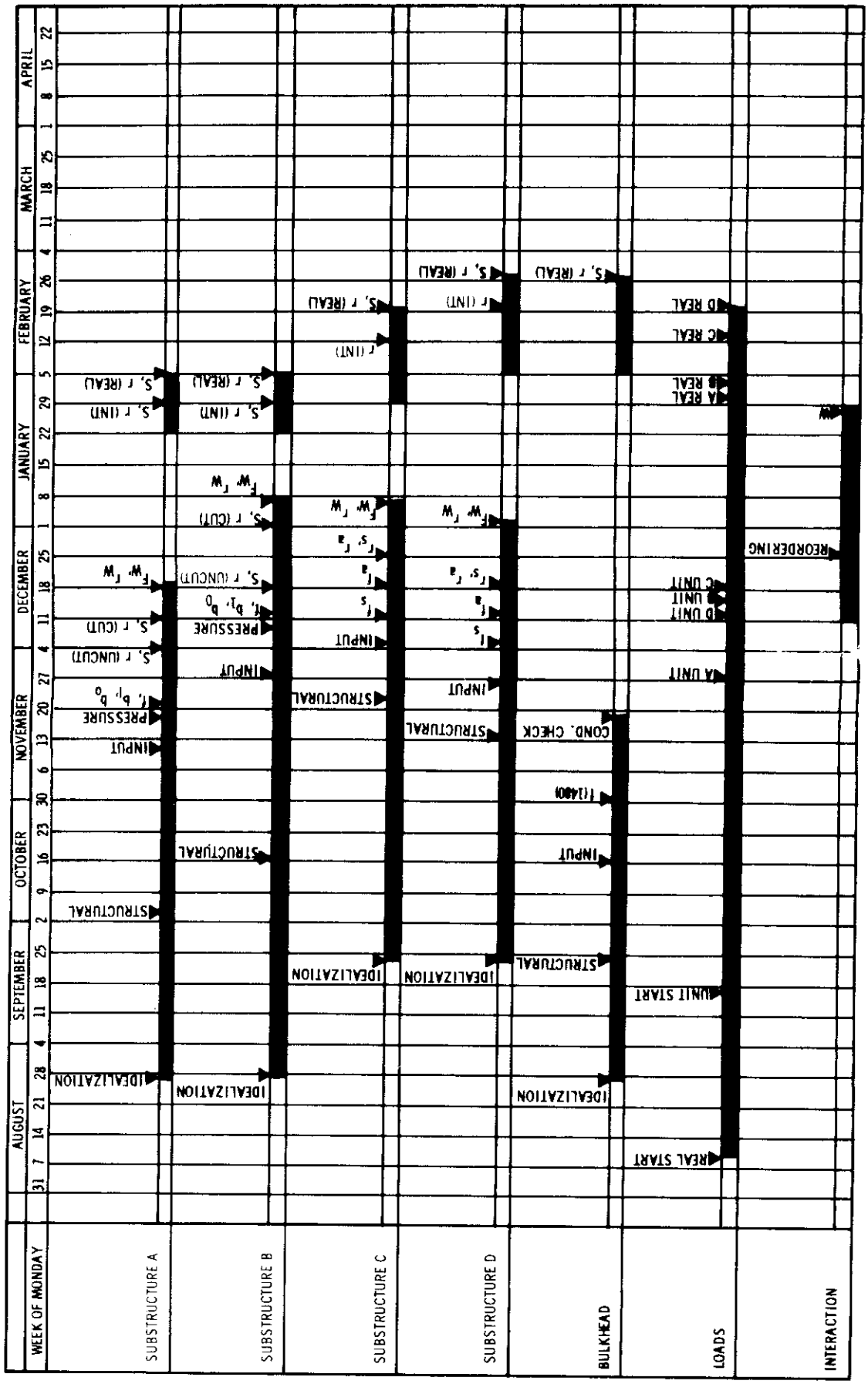

Figure 9. Scheduling Chart

COMPUTER AND MANPOWER RESOURCES

A summary of the CDC 6600 computer requirements is shown below:

Task	Central Processor Time (Hr)	Residency Time (Hr)
Generation of **F** and **r** - Substructure A	3.1	12.8
Generation of **F** and **r** - Substructure B	3.9	15.3
Generation of **F** and **r** - Substructure C	9.8	45.8
Generation of **F** and **r** - Substructure D	6.5	25.7
Interaction Solution	1.9	6.3
Unit solution scaling and output generation	2.3	16.6
Totals	27.5	122.5

A total of 28 hours of central processor time was required for an error-free pass through the system. An additional 50 hours was required, however, for data checkout, new program development and checkout, and recovery from machine and magnetic tape failure.

Manpower requirements were approximately as follows:

- 747 Stress group — 55 man-months
- Stress Analysis Research group — 20 man-months
- Structures Programming group — 18 man-months

SECTION IV

QUALITY OF RESULTS

It is necessary for an analysis of this importance to establish with reasonable certainty that the programs and computers have functioned correctly and that the character of the idealization has not produced ill-conditioned equations and, hence, results that are of poor quality or meaningless. All checks involving the structure are based upon either equilibrium of forces of compatibility of deflections.

A meaningful check on the solution is provided by the compatibility of the substructure interfaces after interaction. Two considerations are important in checking this compatibility. The first and most meaningful to the numerical analyst is the difference between the gaps or lack of closure for the interacting freedoms before and after interaction. This check determines the accuracy with which the equations have been solved. A more meaningful check to the engineer and a better measure of the usefulness of the results is the actual physical magnitude of the gaps remaining after interaction. A summary of the gaps after interaction on all of the substructure interfaces for a typical generalized unit loadcase is shown in Figure 10. As may be seen, the poorest quality closure occurred on the C-D interface. Significantly, substructure D is very flexible at several points along this interface. For example, the largest gap of 0.2 inches occurred in the fore and aft direction at the connection of the landing gear beam to the wing. Since this is an isolated point, the force required to close the gap was easily determined as approximately 50 lb, an insignificant amount. The next largest gap was 0.022 inches, occurring at a soft point on the pressure web. Gaps at the connection of the keel beam chords, a relatively hard area, were of the order of 0.0001 inch, a magnitude of no physical significance.

It is a necessary condition that the internal loads on the structure balance the externally applied loads. A typical equilibrium check was performed by hand at five sections through the combined B and D substructures in the wheel-well region. The results of this check are shown in the following table for three generalized unit loadcases. The sections chosen included the entire structure in the area and were parallel to the body frames. The ratios given are the difference between summed internal members loads and total external applied loads, divided by the total external applied load acting at the section. A large amount of the error is directly attributable to the difficulty in interpolating the results for some irregularly shaped plate elements with boundaries not consistent with the plane of the section being taken. Automatic checks for this type of equilibrium were performed in the monocoque at cross-sections involving only one substructure.

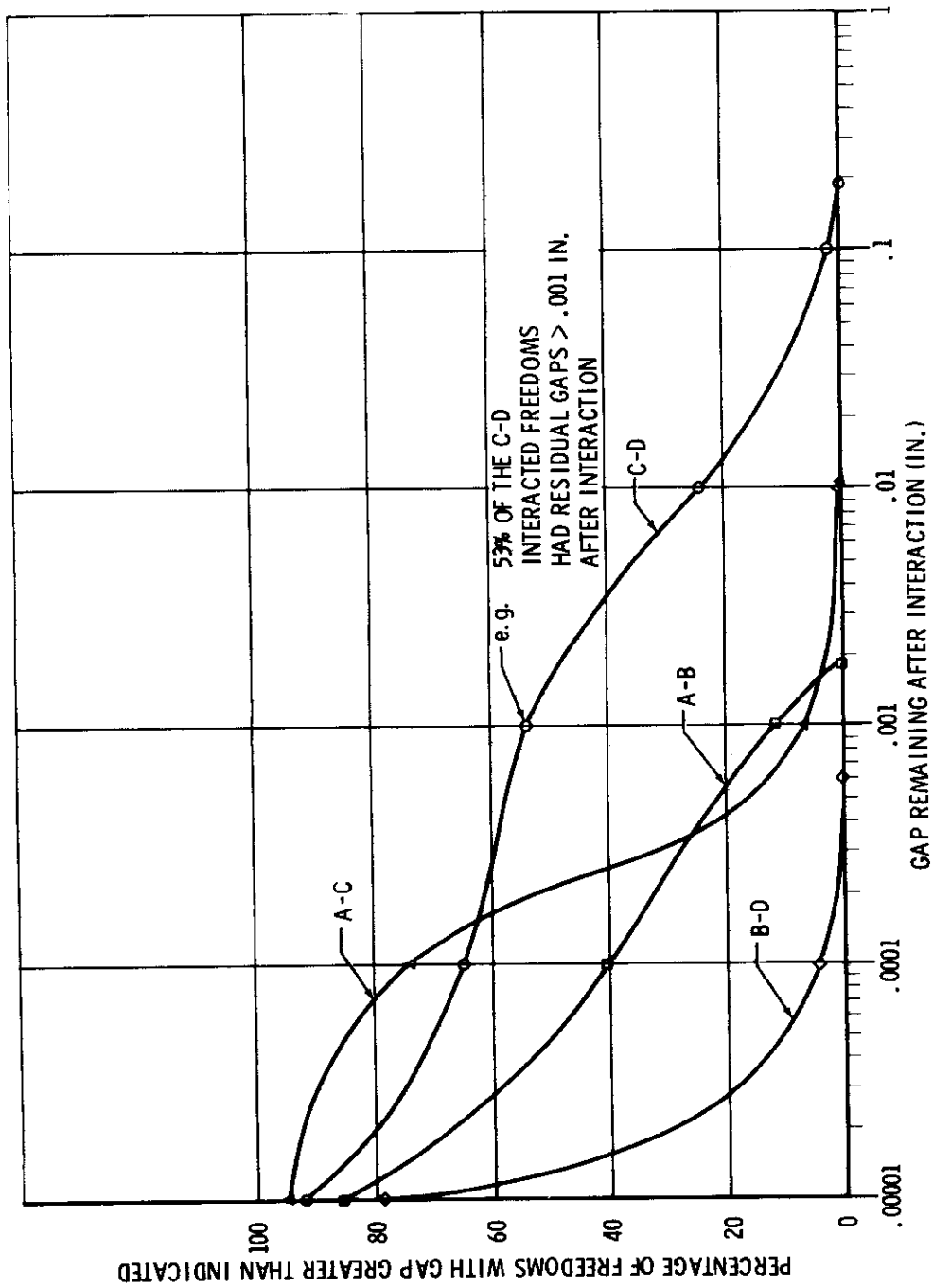

Figure 10. Quality of Closure

Cross-section	Vertical Shear, V_z		Pitching Moment, M_y		Fore and Aft Thrust, V_x	
	$\frac{V_z}{V_z}$	% Error	$\frac{M_y}{M_y}$	% Error	$\frac{V_x}{V_x}$	% Error
1	$\frac{2^{K*}}{375^{K}}$	0.53	$\frac{8^{M**}}{425^{M}}$	1.9	***	
2	$\frac{0}{367^{K}}$	0	$\frac{1.5^{M}}{420^{M}}$	0.36	$\frac{4^{K}}{1,320^{K}}$	0.30
3	$\frac{1^{K}}{324^{K}}$	0.31	$\frac{2.6^{M}}{395^{M}}$	0.66	$\frac{1^{K}}{1,260^{K}}$	0.08
4	$\frac{8^{K}}{605^{K}}$	1.3	$\frac{.146^{M}}{267^{M}}$	0.05	$\frac{0}{1,460^{K}}$	0
5	$\frac{3^{K}}{593^{K}}$	0.51	$\frac{5.6^{M}}{328^{M}}$	1.7	$\frac{6^{K}}{1,220^{K}}$	0.49

Quality of Equilibrium

* 10^3 lb

** 10^6 in.-lb

*** not calculated

Since the structure analyzed was perfectly symmetrical, the symmetry of the results provides a reliable check on the accuracy of the solution. The following list gives a summary of interaction force pairs having a symmetry of 5, 4, 3, 2 and 1 figures, respectively:

Number of Figures of Symmetry	% of Total Force Pairs
5	3.8
4	58.1
3	28.0
2	9.0
1	1.1

An interaction force pair is two symmetrical interaction forces. Symmetry does not take on physical significance, however, unless related to actual force magnitudes. Figure 11 relates the degree of symmetry to force magnitude for a typical generalized unit loadcase. For this particular case, the maximum error in symmetry is approximately 10 lb. whereas the maximum interaction force is about 40,000 lb. This caliber of symmetry was typical of interaction forces, stresses, and deflections.

SECTION V

DISCUSSION OF RESULTS

The purpose of this analysis was to provide detailed internal loads information so that the aircraft structure could be satisfactorily designed to meet or exceed goals in structural performance. The theoretical correctness and practical usefulness of finite element, matrix, and interaction theory have been well established elsewhere. Hence, this discussion is confined to the usefulness of the results for design purposes and the reasons why this expensive and difficult analysis was necessary.

As an illustration of the complexity of the results, cross-section plots of stringer axial loads in the monocoque are given in Figure 12 for symmetrical body bending. For comparison, some stress distributions obtained from a corresponding equilibrium analysis based on an Mc/I distribution are also shown. The panel shear flow distribution for the monocoque for the same body bending condition is shown in Figure 13. The rapidly varying stress and shear flow patterns around the doorway cutout (B.S. 1265), front spar (B.S. 980), and aft wheel-well bulkhead (B.S. 1480) are typical of this type of structure and illustrate the necessity for a redundant analysis. As can be seen, the equilibrium analysis predicts the neutral axis of the structure and the load intensities within reasonable tolerances toward the extremes of the structure where the irregularities have less effect. However, toward the wing-body intersection and wheel-well area, the equilibrium analysis prediction diverges considerably from the redundant analysis predictions. Of course, the equilibrium analysis around irregularities

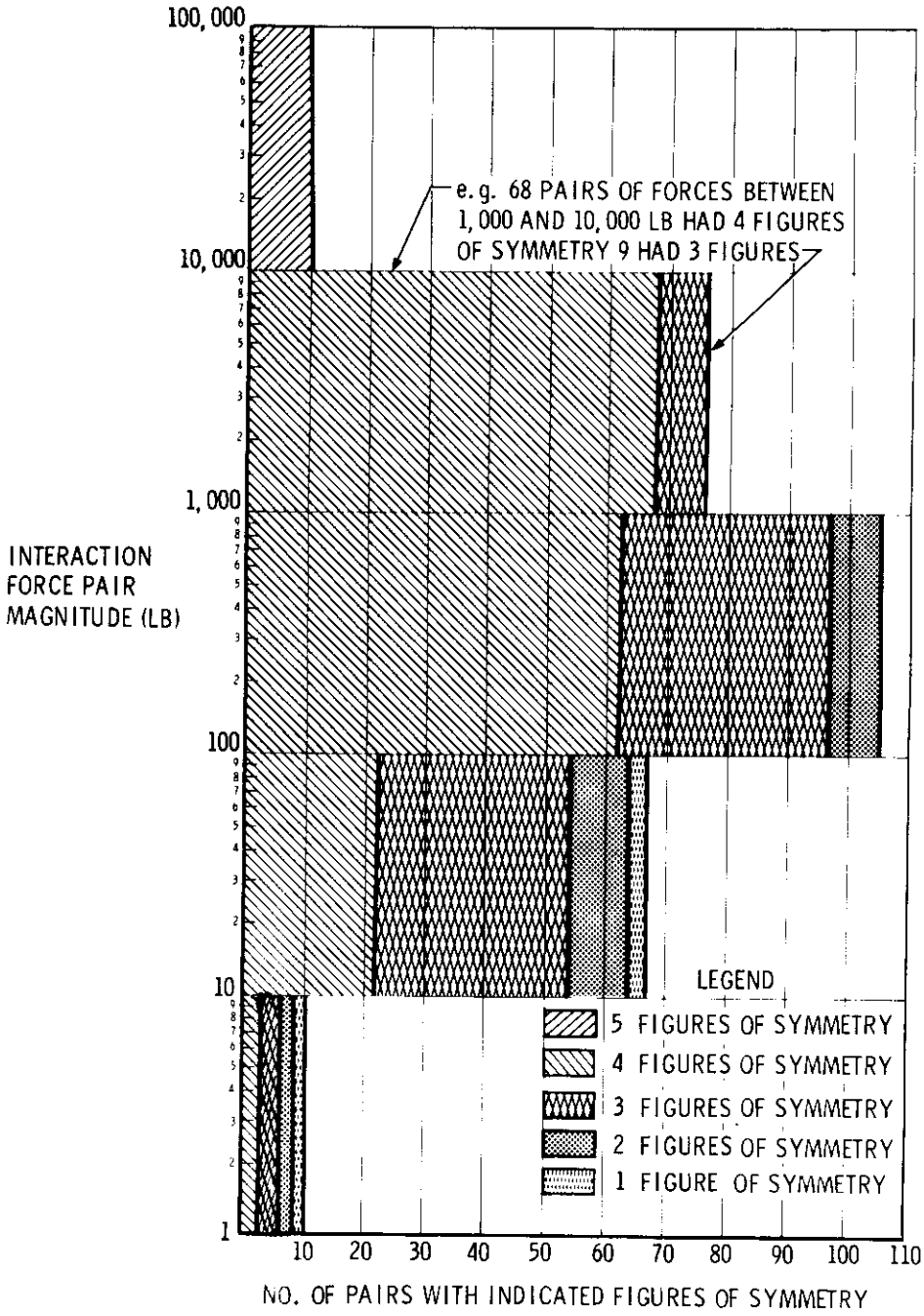

Figure 11. Quality of Symmetry

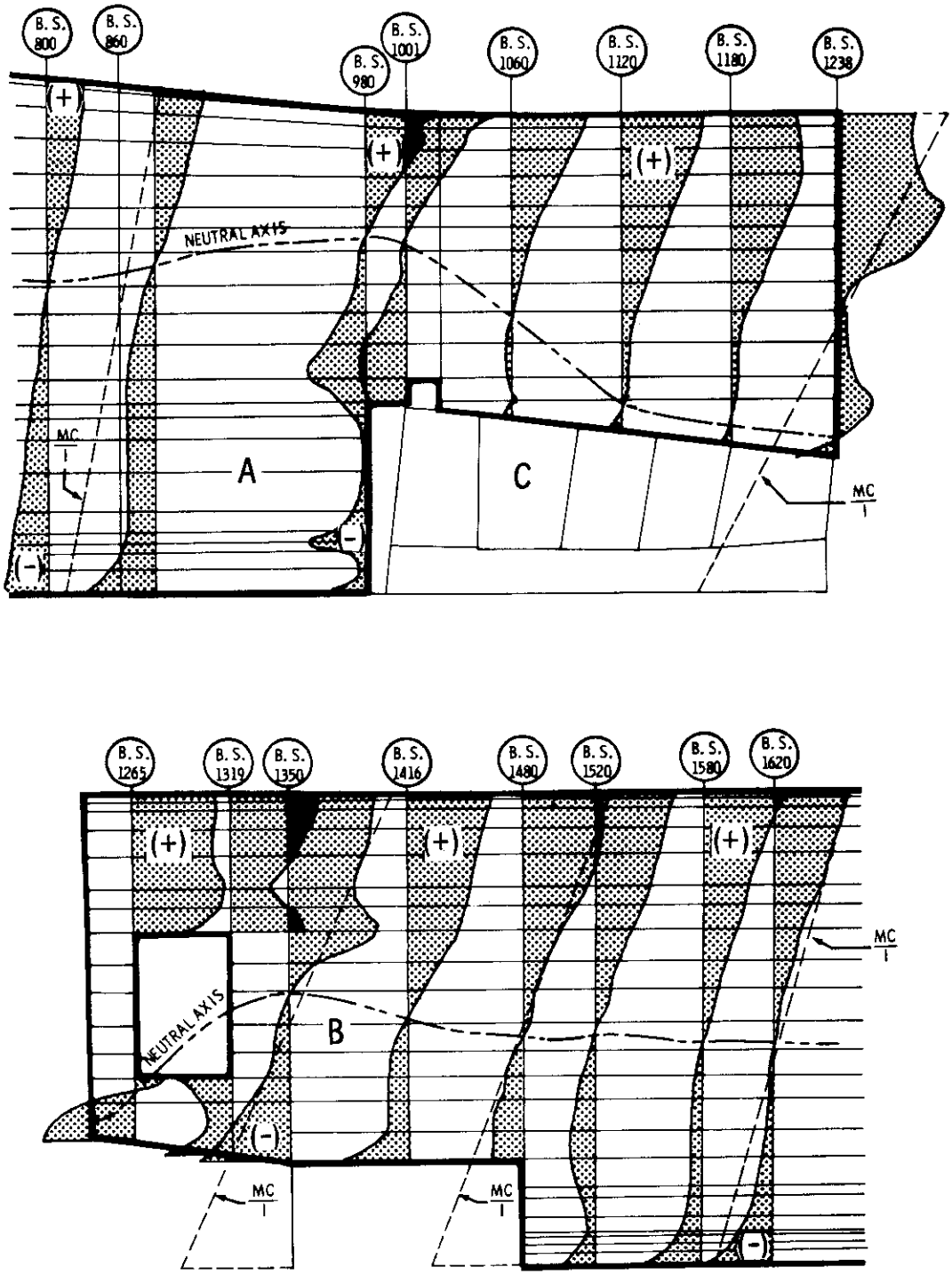

Figure 12. Typical Stringer Axial Stress Plots

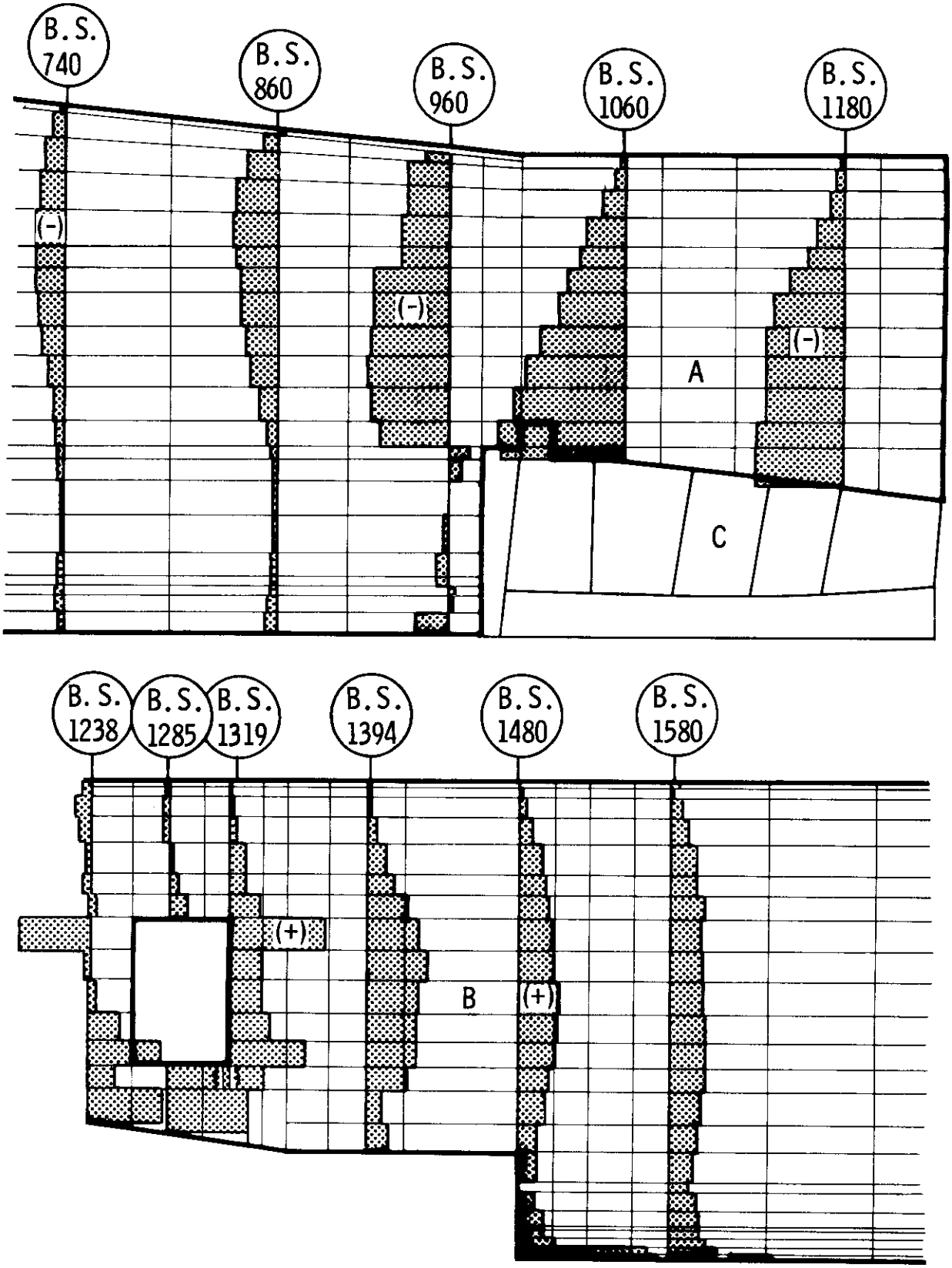

Figure 13. Typical Panel Shear Flow Plots

would be modified in practice, but these modifications would have to be based upon assumed redistributions and effectivities which are difficult to determine. Still, the prediction of loads for static analysis ultimate load design may be satisfactory since the structure is able to adjust itself through local yielding. However, this yielding may produce a questionable fatigue condition.

The useful life of an aircraft can be severely limited by fatigue cracking of primary structural members. Very few areas of the aircraft structure can be designed by ultimate load considerations alone; on the contrary, most areas are affected by fatigue considerations. This is particularly true in the region of the wing-body intersection and the body wheel-well where the constant flexing of the wing, operation of the landing gear, and pressurization of the monocoque cause repeated cycling of loads. The result of this cycling can be fatigue cracking of wing skins, of stub frames along the wing-to-body joint, and of critical splices and connections throughout the region. The nonlinear characteristic of the S-n curve, commonly used in fatigue analysis, indicates that even a very small increase in static load may result in a disproportionate reduction in the fatigue life of a structural member operating near yield. Hence, design for fatigue requires a more detailed and exact knowledge of internal loads than is required for ultimate load design.

Figure 14 is a view of the upper arch of the rear spar bulkhead at B.S. 1238 showing the shear flow pattern for a symmetrical body bending condition. The normal dissipation of shear flow from the overwing longeron to the monocoque crown is disturbed by the effect of the passenger access door aft of the bulkhead (Figure 13).

The loads in the mid wheel-well bulkhead (B.S. 1350), for a ground maneuver condition are shown in Figure 15. This bulkhead is located behind the rear spar with the landing gear beams cantilevered from each side projecting outward to intersect the wing rear spar. The purpose of the beams is to support the outboard landing gear and to carry some of the wing flight loads. Consequently, one of the loads carried by the bulkhead is induced by the relative displacement of the bulkhead as part of the aft body compared to the deflection at the point of intersection of the landing gear beam and the rear spar.

Figure 15 gives an example of the axial load distribution in the chords of this bulkhead resulting from loading the landing gear beam. The very rapid change of load in the mid chord and the corresponding rapid changes in the upper and lower chords produce extremely high shear values in the outboard plates. Because of the fineness of the grid, however, the solution

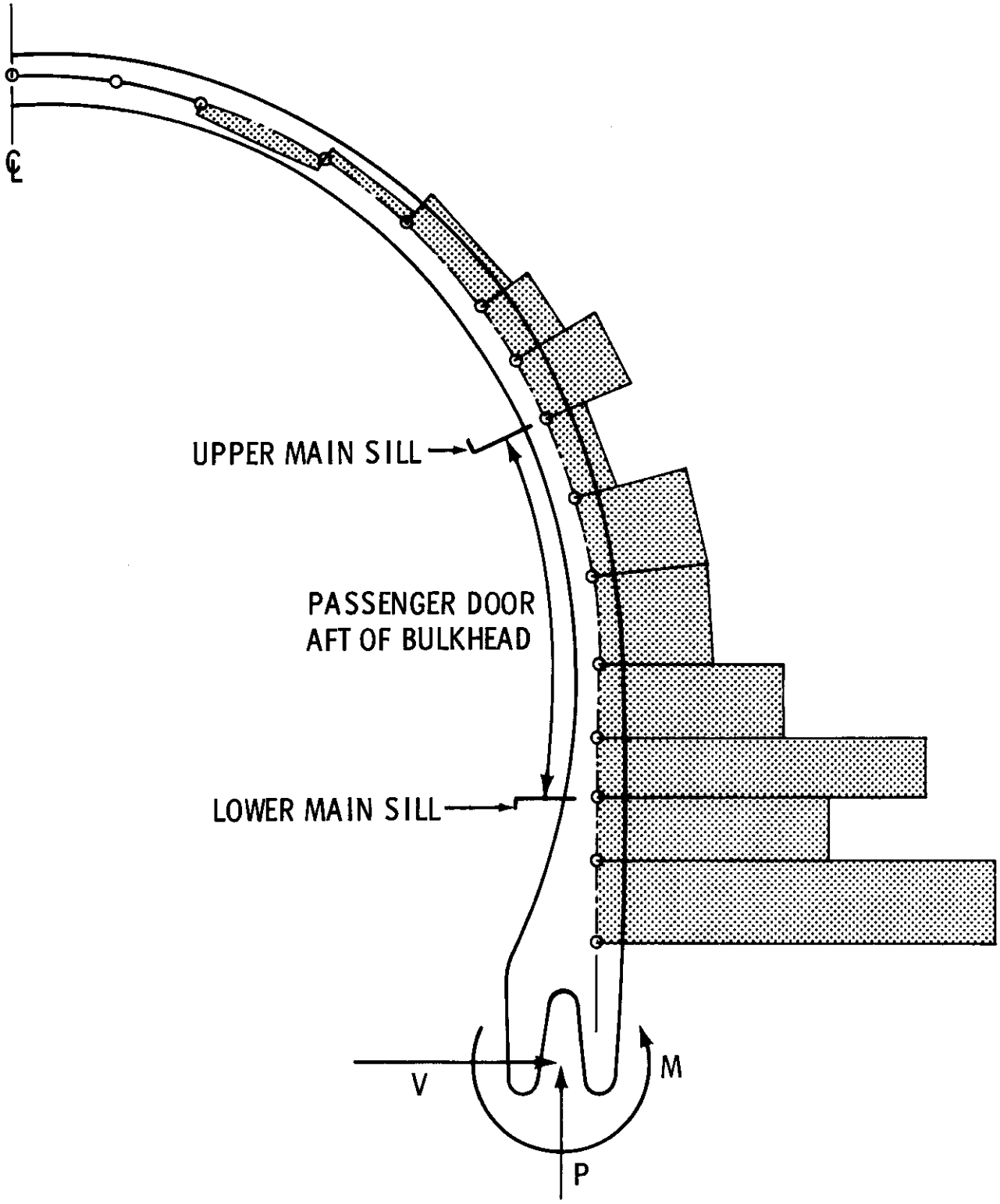

Figure 14. Rear Spar Bulkhead Arch - Shear Flow Distribution

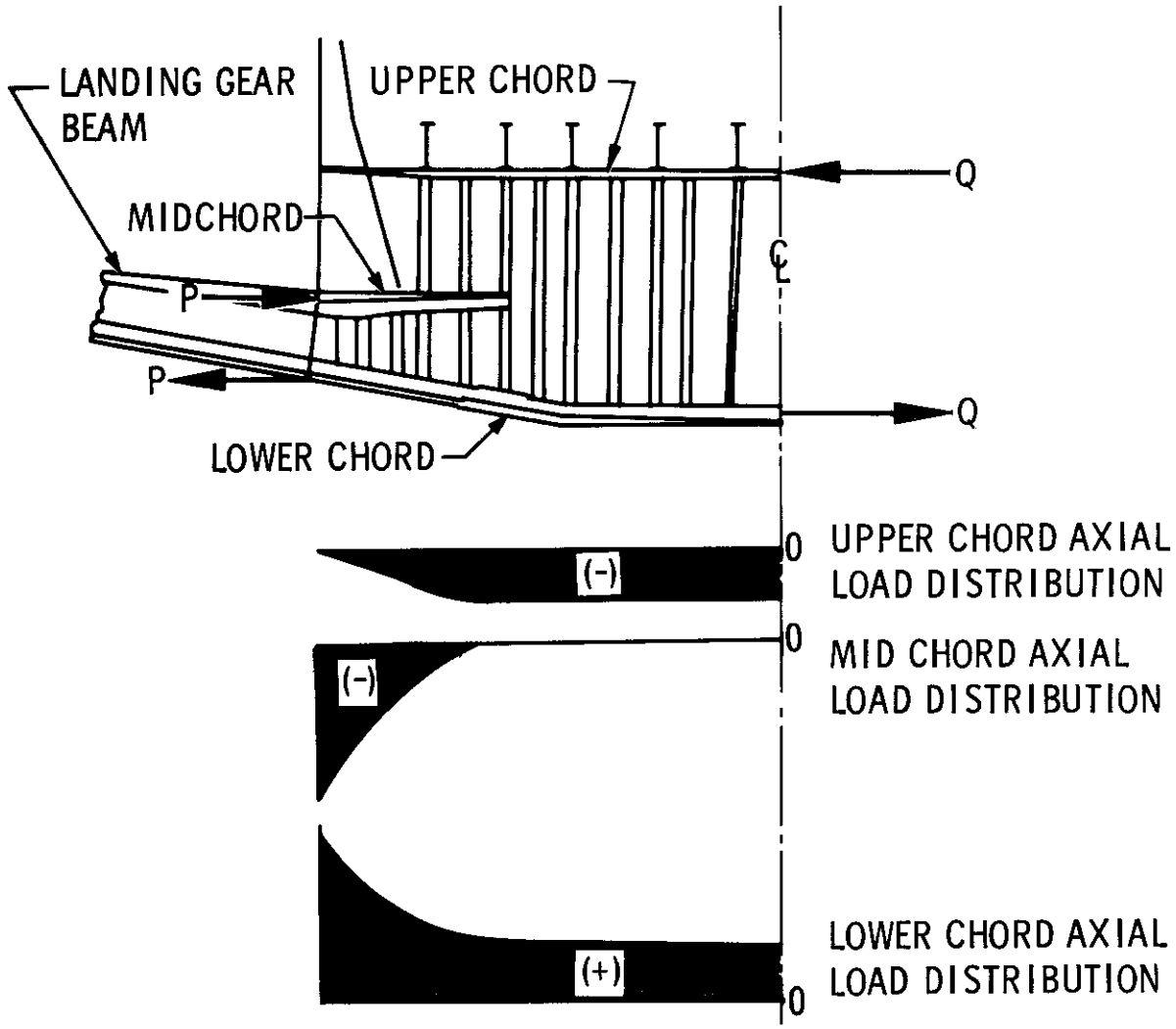

Figure 15. B.S. 1350 Bulkhead Load Distribution

was able to provide knowledge suitable for detail design of this highly critical area. A further benefit from the analysis in this particular region was the accurate determination of the percentage of wing load carried by the landing gear beam. The redundance introduced by cantilevering the landing gear beam from the bulkhead would have made this determination extremely difficult, if not impossible, using less sophisticated analysis techniques.

Figure 16 illustrates the loads on the B.S. 1480 bulkhead for a symmetrical ground maneuver condition. It shows the landing gear loads and the balancing shear forces around the bulkhead in addition to the shear flows caused by redistribution of aft monocoque loads around the wheel-well cutout.

A very useful result not available from an equilibrium analysis is the accurate prediction of displacements required for control routing, fit, and correct working of mechanical gear.

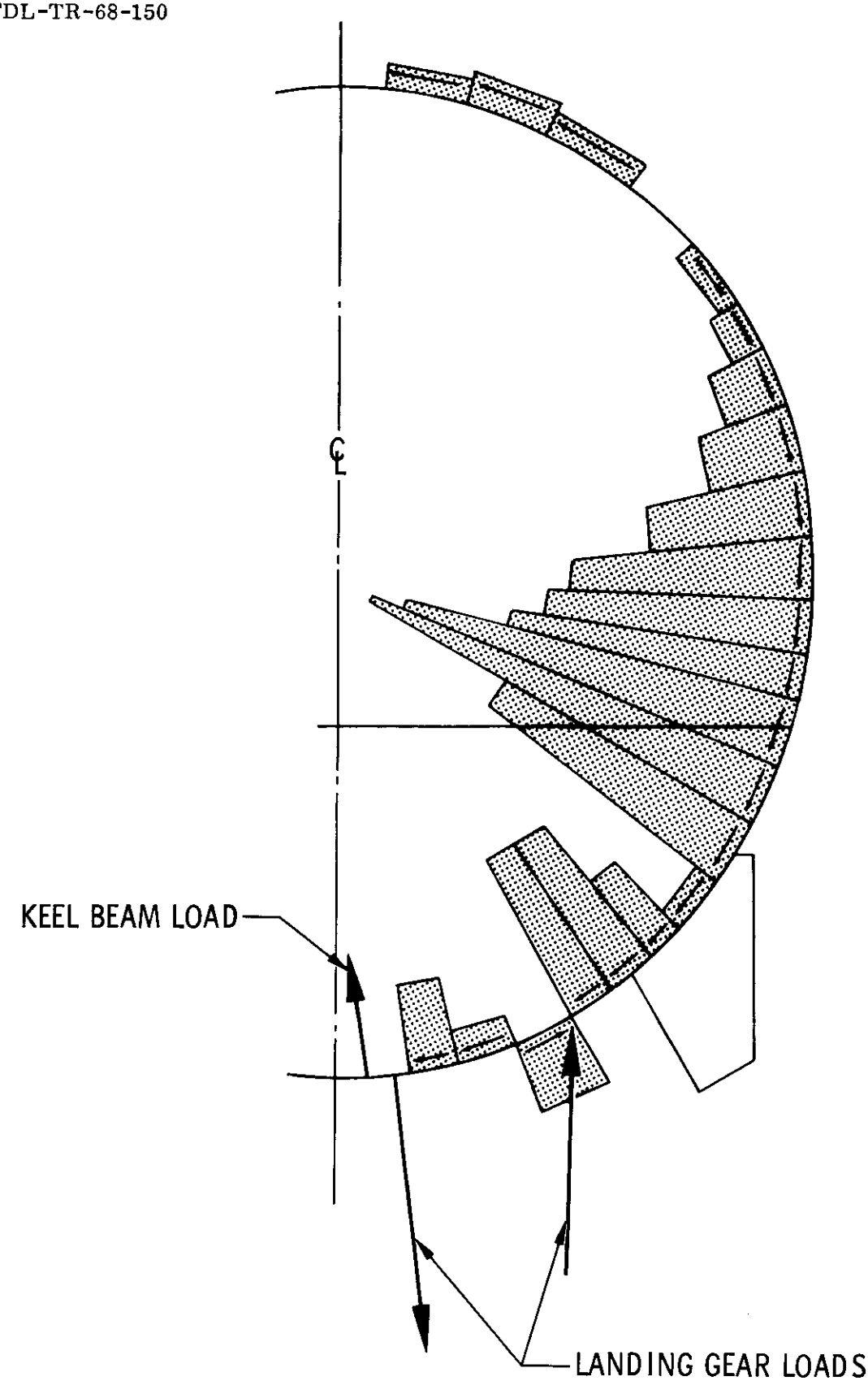

Figure 16. B.S. 1480 Bulkhead Shear Force Distribution

Many subjective results have been derived from the analysis. Some of these are as follows.

- Treatment of the wing-body intersection region as a single structure eliminated the necessity for overlapping design assumptions at the interface of major structural components.

- Applied loads were consistent and balanced over the entire region.

- A common working technical language was established between company groups and between the company and its subcontractors working on this region.

- A common base for the total wing-body design effort was established, eliminating inconsistent analysis procedures and the resulting frustrations.

- Accurate prediction of internal static loads on a detailed basis provided data for fatigue analysis normally not available until static test or later.

- Parametric studies using the stresses and deflections from the generalized unit loadcases can provide insight into the behavior of the structure that will be invaluable during development of future aircraft.

The final and most critical test of this analysis will be the performance of the aircraft when placed in service with the world's airlines. However, it is expected that the knowledge provided has already resulted in a more efficient structure with reduced weight and improved service life.

SECTION VI

REFERENCES

1. J. H. Argyris and S. Kelsey, Modern Fuselage Analysis and Elastic Aircraft Butterworth, London, 1962.

2. M. J. Turner, R. W. Clough, H. C. Martin, and L. J. Topp, "Stiffness and Deflection Analysis of Complex Structures," Journal of Aeronautical Science, Vol. 23, No. 9, 1956.

3. J. S. Przemieniecki and P. H. Denke, "Joining of Complex Structures by the Matrix Force Method," Journal of Aircraft, Vol. 3, No. 3, 1966.

APPENDIX

747 CARGO DOOR-CABIN INTERACTION ANALYSIS

The region of the 747 analyzed in this project was the cross-hatched area at the nose of aircraft shown in Figure 1. The objective of this analysis was to obtain door hinge and latch loads at the interface between the cargo door and the body. To accomplish this task the area was idealized as two substructures (Figure 17). A flexibility-type interaction analysis was chosen, since the direct output from the solution of the interaction equations would be the door hinge and latch loads. Further, a failsafe analysis of the door hinges and latches could be easily and economically accomplished. This involved striking out the row and column in the flexibility matrix corresponding to the load freedom that was assumed to have failed and resolving the interaction equations. Noteworthy is the fact that the door latches were oriented tangential to the fuselage surface, requiring a unique freedom orientation at each interacting node. The analysis was completed for design of the cargo version of the 747. The statistics are as follows.

Substructure	Nodes	Simultaneous Equations	Interaction Forces
1	894	2,680	42
2	425	1,250	

727 WING-BODY INTERACTION ANALYSIS

The 727-200 wing-body interaction analysis used the same system of programs, and was approached in essentially the same manner as that for the 747-4 aircraft. The region analyzed was the shaded area shown in Figure 18. A schematic of the three substructures involved showing their relative sizes and position is given in Figure 19. A summary of statistics follows.

Substructure	Nodes	Simultaneous Equations	Interaction Forces
A	1,500	1,470	A-B,C 167
B	1,200	1,100	A-B 105
C	570	3,400	A-C 62

One essential difference between the 727 analysis and that of the 747 is that the 727 wing was idealized as a complete structure rather than as a symmetric half structure. An equally important difference was that the wing of the 727 aircraft is pinned to the fuselage rather than rigidly connected as is the case with the 747 wing. The 727 wind connection greatly reduced the number of interaction freedoms between the wing and body.

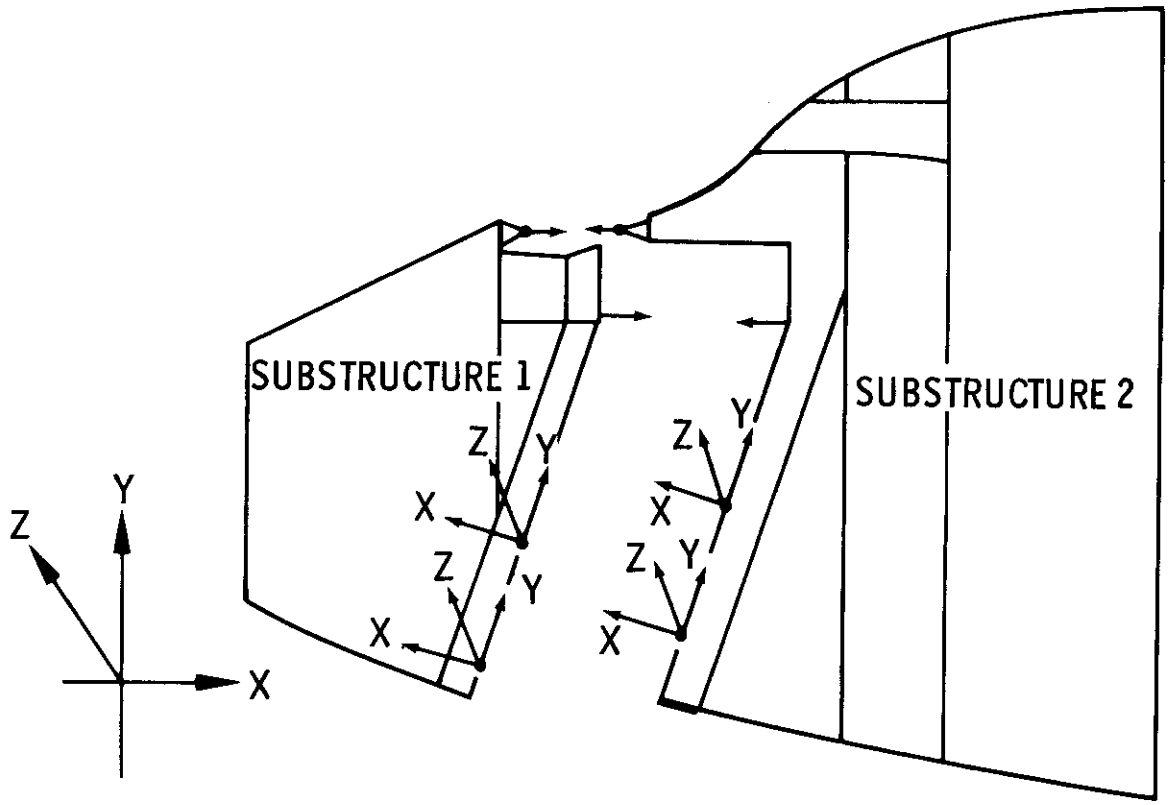

Figure 17. 747 Cargo Door and Cabin

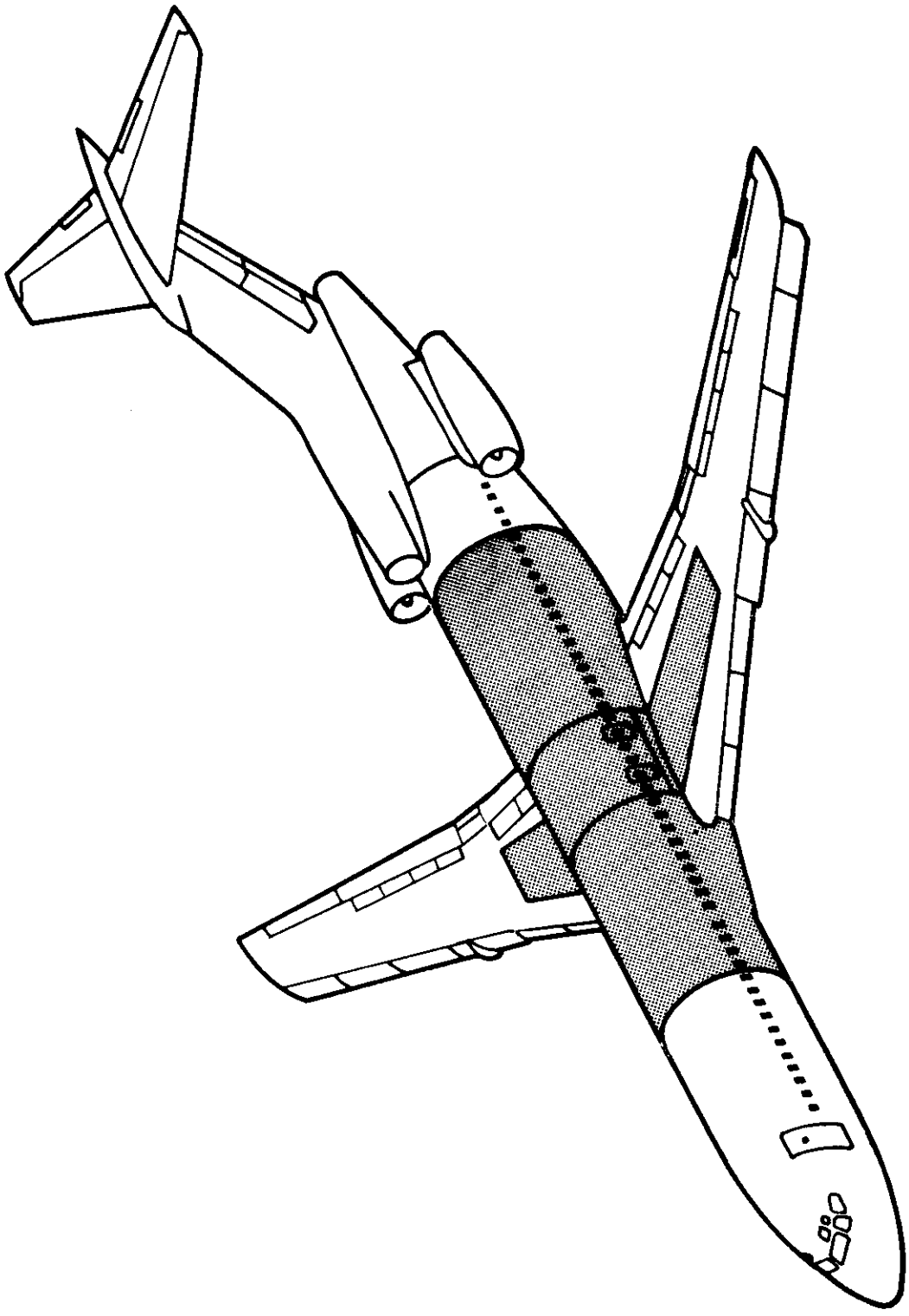

Figure 18. 727 Wing-Body Intersection - Region Analyzed

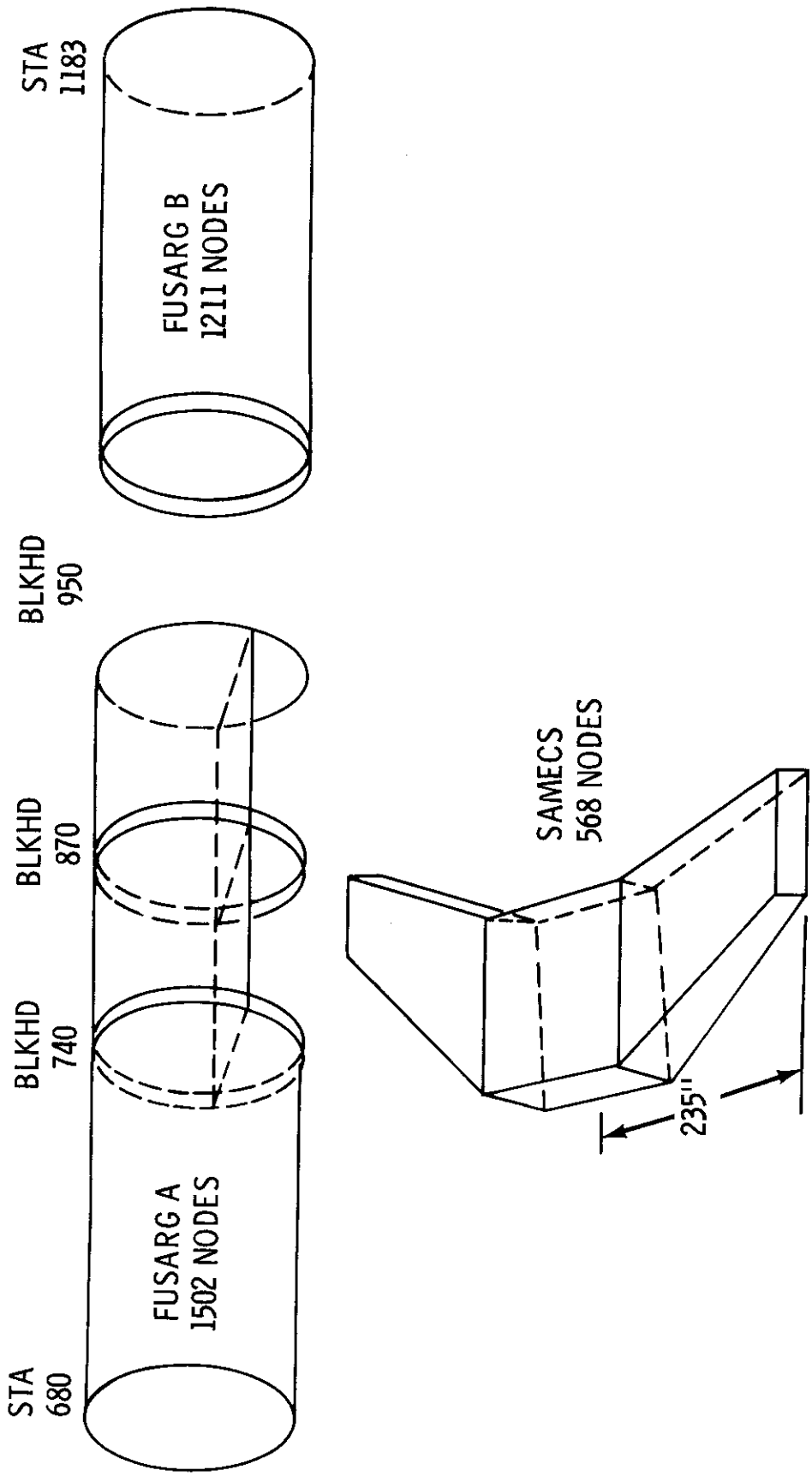

Figure 19. 727 Wing-Body Intersection - Substructure Schematic